of TRAP-positive and trypan blue-negative osteoclasts was counted.

Real-time quantitative RT-PCR

Total RNA was extracted with ISOGEN (Wako Pure Chemical), and an aliquot (1 μg) was reverse-transcribed using a PrimeScript RT reagent Kit (Takara Bio) to make single-stranded cDNA. PCR was performed on an ABI Prism 7000 Sequence Detection System (Applied Biosystems) using QuantiTect SYBR Green PCR Master Mix (QIAGEN) according to the manufacturer's instructions. All reactions were run in triplicate. After data collection, the mRNA copy number of a specific gene in total RNA was calculated with a standard curve generated with serially diluted plasmids containing PCR amplicon sequences, and normalized to the rodent total RNA (Applied Biosystems) with mouse β-actin as an internal control. Standard plasmids were synthesized with a TOPO TA Cloning Kit (Invitrogen), according to the manufacturer's instruction. Primer sequences are stated in the Supporting Protocol S1 online.

Western blot analyses

Cells were washed twice with ice-cold PBS, and proteins were extracted with M-PER (Pierce Chemical) or NE-PER (Pierce Chemical), according to the manufacturer's instructions. To detect the phosphorylation of FoxO3a, the lysates were treated with lambda protein phosphatase (New England Bio Labs). For Western blot analysis, lysates were fractionated by SDS-PAGE with 7.5–15% Tris-Glycin gradient gel or 15% Tris-Glycin gel, and transferred onto nitrocellulose membranes (BIO-RAD). After blocking with 6% milk/TBS-T, membranes were incubated with primary antibodies to pan-Akt, phospho-Akt, Akt1, Akt2, FoxO1, cleaved caspase-3, Bax, Bcl-2 (Cell Signaling Technology), FoxO3a (Upstate), Bim (BD Parmingen), Bcl-x_L (Santa Cruz Biotechnology), and β-actin (Sigma-Aldrich), followed with HRP-conjugated goat anti-mouse IgG and goat anti-rabbit IgG (Promega). Immunoreactive bands were visualized with ECL Plus (Amersham), according to the manufacturer's instructions.

Luciferase assays

MC3T3-E1 cells were plated onto 24-well plates, then subsequently transfected in triplicate with 0.1 μg of the reporter plasmid, 0.2 μg of effector plasmids, and 8 ng of pRL-TK vector (Promega) for internal control, by using FuGENE6 (Roche Diagnostics). The amount of total DNA in each well was adjusted to be equal. Details are described in Supporting Protocol S1 online. The luciferase assay was performed 48 h after transfection with a dual-luciferase reporter assay system and GloMax™ 96 Microplate Luminometer (Promega). Firefly output was normalized to Renilla output to control for transfection efficiency.

ChIP assay

ChIP assay was performed with a ChIP Assay Kit (Upstate), according to the manufacturer's instructions. PCR was performed to amplify the promoter region (−471/−67) of osteocalcin gene containing the OSE2 site which Runx2 is reported to bind [40]. Primer sequences are given in Supporting Protocol S1 online.

Statistical analyses

Means of groups were compared by ANOVA and significance of differences was determined by post-hoc testing with Bonferroni's method.

SUPPORTING INFORMATION

Figure S1 Phosphorylation and expression pattern of Akt isoforms in bone cells. (A) Time course of phosphorylated total Akt (P-Akt) and total Akt (Akt) levels determined by Western blotting in cultured mouse calvarial osteoblasts (OB) after stimulation with IGF-I or BMP-2, and in cultured bone marrow macrophages (BMM) and mature osteoclasts (OC) after stimulation with M-CSF. (B) Expressions of each Akt isoform in the cells above determined by quantitative real-time RT-PCR analysis using the same amount of template cDNA. Data are expressed as means (bars)±SEM (error bars) of the relative amount of mRNA as compared to that of Akt1.
Found at: doi:10.1371/journal.pone.0001058.s001 (0.49 MB TIF)

Figure S2 Akt1-/- mice showed growth retardation. (A) Body weight and naso-anal length of WT (+/+) and Akt1-/- littermates. Data are expressed as means (symbols)±SEM (error bars) for 4–10 mice/group. *P<0.05 vs. WT. (B) Plain X-ray images of the whole body of representative male littermates at 8 weeks of age. Bar, 1 cm.
Found at: doi:10.1371/journal.pone.0001058.s002 (1.47 MB TIF)

Figure S3 FoxO3a translocated into nucleus after serum deprivation. Time course of subcellular localization of GFP-tagged FoxO3a after serum deprivation in MC3T3-E1 cells. Bar, 20 μm.
Found at: doi:10.1371/journal.pone.0001058.s003 (2.16 MB TIF)

Figure S4 Effects of Actinomycin D, insulin, and IGF-I on Bim expression after serum deprivation. (A) Time course of Bim mRNA level determined by real-time RT-PCR after serum deprivation in cultured calvarial osteoblasts with and without Actinomycin D (1 μM). Data are normalized to those of β-actin and are expressed as means (symbols)±SEM (error bars) of the relative amount compared to time 0. (B) Time course of Bim protein level determined by Western blotting after serum deprivation in cultured calvarial osteoblasts with and without Actinomycin D (1 μM). (C) Time course of Bim mRNA level determined by real-time RT-PCR after serum deprivation in cultured calvarial osteoblasts with and without insulin (100 nM), IGF-I (10 nM), or FBS (10%). Data are normalized to those of β-actin and are expressed as means (symbols)±SEM (error bars) of the relative amount compared to time 0.
Found at: doi:10.1371/journal.pone.0001058.s004 (0.38 MB TIF)

Figure S5 Akt1 did not affect osteoblastic differentiation of immature mesenchymal cell lines. ALP staining of cultured C2C12 cells and C3H10T1/2 cells that were adenovirally transfected with GFP, $Akt1^{CA}$, or Runx2.
Found at: doi:10.1371/journal.pone.0001058.s005 (1.52 MB TIF)

Protocol S1
Found at: doi:10.1371/journal.pone.0001058.s006 (0.10 MB DOC)

ACKNOWLEDGMENTS

We are grateful to Drs. H. Katagiri and T. Asano for adenovirus expressing $Akt1^{CA}$, Dr. H. Takayanagi for luciferase reporter constructs containing osteocalcin promoter region, and Dr. R. Nishimura for adenovirus expressing Runx2.

Author Contributions

Conceived and designed the experiments: HK NK FK TA KN UC. Performed the experiments: NK FK YO SO TI TS YK YS YA. Analyzed the data: HK NK FK TI NO KH TA KN UC ST. Contributed reagents/materials/analysis tools: NH TK YO KT ST WC. Wrote the paper: HK NK.

REFERENCES

1. Harada S, Rodan GA (2003) Control of osteoblast function and regulation of bone mass. Nature 423: 349–355.
2. Boyle WJ, Simonet WS, Lacey DL (2003) Osteoclast differentiation and activation. Nature 423: 337–342.
3. Thrailkill KM, Lumpkin CK Jr, Bunn RC, Kemp SF, Fowlkes JL (2005) Is insulin an anabolic agent in bone? Dissecting the diabetic bone for clues. Am J Physiol Endocrinol Metab 289: E735–745.
4. Niu T, Rosen CJ (2005) The insulin-like growth factor-I gene and osteoporosis: a critical appraisal. Gene 361: 38–56.
5. Krishnan V, Bryant HU, Macdougald OA (2006) Regulation of bone mass by Wnt signaling. J Clin Invest 116: 1202–1209.
6. Chen D, Zhao M, Mundy GR (2004) Bone morphogenetic proteins. Growth Factors 22: 233–241.
7. Almeida M, Han L, Bellido T, Manolagas SC, Kousteni S (2005) Wnt proteins prevent apoptosis of both uncommitted osteoblast progenitors and differentiated osteoblasts by beta-catenin-dependent and -independent signaling cascades involving Src/ERK and phosphatidylinositol 3-kinase/AKT. J Biol Chem 280: 41342–41351.
8. Ghosh-Choudhury N, Abboud SL, Nishimura R, Celeste A, Mahimainathan L, et al. (2002) Requirement of BMP-2-induced phosphatidylinositol 3-kinase and Akt serine/threonine kinase in osteoblast differentiation and Smad-dependent BMP-2 gene transcription. J Biol Chem 277: 33361–33368.
9. Hanada M, Feng J, Hemmings BA (2004) Structure, regulation and function of PKB/AKT–a major therapeutic target. Biochim Biophys Acta 1697: 3–16.
10. Yang ZZ, Tschopp O, Hemmings-Mieszczak M, Feng J, Brodbeck D, et al. (2003) Protein kinase B alpha/Akt1 regulates placental development and fetal growth. J Biol Chem 278: 32124–32131.
11. Chen WS, Xu PZ, Gottlob K, Chen ML, Sokol K, et al. (2001) Growth retardation and increased apoptosis in mice with homozygous disruption of the Akt1 gene. Genes Dev 15: 2203–2208.
12. Cho H, Mu J, Kim JK, Thorvaldsen JL, Chu Q, et al. (2001) Insulin resistance and a diabetes mellitus-like syndrome in mice lacking the protein kinase Akt2 (PKB beta). Science 292: 1728–1731.
13. Garofalo RS, Orena SJ, Rafidi K, Torchia AJ, Stock JL, et al. (2003) Severe diabetes, age-dependent loss of adipose tissue, and mild growth deficiency in mice lacking Akt2/PKB beta. J Clin Invest 112: 197–208.
14. Peng XD, Xu PZ, Chen ML, Hahn-Windgassen A, Skeen J, et al. (2003) Dwarfism, impaired skin development, skeletal muscle atrophy, delayed bone development, and impeded adipogenesis in mice lacking Akt1 and Akt2. Genes Dev 17: 1352–1365.
15. Kim R (2005) Unknotting the roles of Bcl-2 and Bcl-xL in cell death. Biochem Biophys Res Commun 333: 336–343.
16. Accili D, Arden KC (2004) FoxOs at the crossroads of cellular metabolism, differentiation, and transformation. Cell 117: 421–426.
17. Tran H, Brunet A, Griffith EC, Greenberg ME (2003) The many forks in FOXO's road. Sci STKE 2003: RE5.
18. Liu X, Bruxvoort KJ, Zylstra CR, Liu J, Cichowski R, et al. (2007) Lifelong accumulation of bone in mice lacking Pten in osteoblasts. Proc Natl Acad Sci U S A 104: 2259–2264.
19. Hosaka T, Biggs WH 3rd, Tieu D, Boyer AD, Varki NM, et al. (2004) Disruption of forkhead transcription factor (FOXO) family members in mice reveals their functional diversification. Proc Natl Acad Sci U S A 101: 2975–2980.
20. Huang DC, Strasser A (2000) BH3-Only proteins-essential initiators of apoptotic cell death. Cell 103: 839–842.
21. Dijkers PF, Birkenkamp KU, Lam EW, Thomas NS, Lammers JW, et al. (2002) FKHR-L1 can act as a critical effector of cell death induced by cytokine withdrawal: protein kinase B-enhanced cell survival through maintenance of mitochondrial integrity. J Cell Biol 156: 531–542.
22. Dijkers PF, Medema RH, Lammers JW, Koenderman L, Coffer PJ (2000) Expression of the pro-apoptotic Bcl-2 family member Bim is regulated by the forkhead transcription factor FKHR-L1. Curr Biol 10: 1201–1204.
23. Gilley J, Coffer PJ, Ham J (2003) FOXO transcription factors directly activate bim gene expression and promote apoptosis in sympathetic neurons. J Cell Biol 162: 613–622.
24. Willis SN, Adams JM (2005) Life in the balance: how BH3-only proteins induce apoptosis. Curr Opin Cell Biol 17: 617–625.
25. Akiyama T, Bouillet P, Miyazaki T, Kadono Y, Chikuda H, et al. (2003) Regulation of osteoclast apoptosis by ubiquitylation of proapoptotic BH3-only Bcl-2 family member Bim. Embo J 22: 6653–6664.
26. Jilka RL, Weinstein RS, Bellido T, Parfitt AM, Manolagas SC (1998) Osteoblast programmed cell death (apoptosis): modulation by growth factors and cytokines. J Bone Miner Res 13: 793–802.
27. Fujita T, Azuma Y, Fukuyama R, Hattori Y, Yoshida C, et al. (2004) Runx2 induces osteoblast and chondrocyte differentiation and enhances their migration by coupling with PI3K-Akt signaling. J Cell Biol 166: 85–95.
28. Lee ZH, Kim HH (2003) Signal transduction by receptor activator of nuclear factor kappa B in osteoclasts. Biochem Biophys Res Commun 305: 211–214.
29. Wong BR, Besser D, Kim N, Arron JR, Vologodskaia M, et al. (1999) TRANCE, a TNF family member, activates Akt/PKB through a signaling complex involving TRAF6 and c-Src. Mol Cell 4: 1041–1049.
30. Sugatani T, Hruska KA (2005) Akt1/Akt2 and mammalian target of rapamycin/Bim play critical roles in osteoclast differentiation and survival, respectively, whereas Akt is dispensable for cell survival in isolated osteoclast precursors. J Biol Chem 280: 3583–3589.
31. Rosen CJ, Dimai HP, Vereault D, Donahue LR, Beamer WG, et al. (1997) Circulating and skeletal insulin-like growth factor-I (IGF-I) concentrations in two inbred strains of mice with different bone mineral densities. Bone 21: 217–223.
32. Liu JP, Baker J, Perkins AS, Robertson EJ, Efstratiadis A (1993) Mice carrying null mutations of the genes encoding insulin-like growth factor I (Igf-1) and type 1 IGF receptor (Igf1r). Cell 75: 59–72.
33. Canalis E, Centrella M, Burch W, McCarthy TL (1989) Insulin-like growth factor I mediates selective anabolic effects of parathyroid hormone in bone cultures. J Clin Invest 83: 60–65.
34. Yamaguchi M, Ogata N, Shinoda Y, Akune T, Kamekura S, et al. (2005) Insulin receptor substrate-1 is required for bone anabolic function of parathyroid hormone in mice. Endocrinology 146: 2620–2628.
35. Ohlsson C, Bengtsson BA, Isaksson OG, Andreassen TT, Slootweg MC (1998) Growth hormone and bone. Endocr Rev 19: 55–79.
36. Huang BK, Golden LA, Tarjan G, Madison LD, Stern PH (2000) Insulin-like growth factor I production is essential for anabolic effects of thyroid hormone in osteoblasts. J Bone Miner Res 15: 188–197.
37. Yamada T, Kawano H, Koshizuka Y, Fukuda T, Yoshimura K, et al. (2006) Carminerin contributes to chondrocyte calcification during endochondral ossification. Nat Med 12: 665–670.
38. Parfitt AM, Drezner MK, Glorieux FH, Kanis JA, Malluche H, et al. (1987) Bone histomorphometry: standardization of nomenclature, symbols, and units. Report of the ASBMR Histomorphometry Nomenclature Committee. J Bone Miner Res 2: 595–610.
39. Akune T, Ogata N, Hoshi K, Kubota N, Terauchi Y, et al. (2002) Insulin receptor substrate-2 maintains predominance of anabolic function over catabolic function of osteoblasts. J Cell Biol 159: 147–156.
40. Ducy P, Karsenty G (1995) Two distinct osteoblast-specific cis-acting elements control expression of a mouse osteocalcin gene. Mol Cell Biol 15: 1858–1869.

THE JOURNAL OF BIOLOGICAL CHEMISTRY VOL. 282, NO. 49, pp. 35757–35764, December 7, 2007

Continuous Activation of $G\alpha_q$ in Osteoblasts Results in Osteopenia through Impaired Osteoblast Differentiation*

Received for publication, December 29, 2006, and in revised form, September 5, 2007 Published, JBC Papers in Press, September 5, 2007, DOI 10.1074/jbc.M611902200

Naoshi Ogata[‡§], **Hiroshi Kawaguchi**[§1], **Ung-il Chung**[§], **Sanford I. Roth**[¶], **and Gino V. Segre**[‡]

From the [‡]*Endocrine Unit and* [¶]*Pathology, Massachusetts General Hospital, Harvard Medical School, Boston, Massachusetts 02114 and* [§]*Sensory & Motor System Medicine, Faculty of Medicine, University of Tokyo, Tokyo 113-8655, Japan*

We explored the role of $G\alpha_q$-mediated signaling on skeletal homeostasis by selectively expressing a constitutively active $G\alpha_q$ (mutation of Q209L) in osteoblasts. Continuous signaling via $G\alpha_q$ in mouse osteoblastic MC3T3-E1 cells impaired differentiation. Mice that expressed the constitutively active $G\alpha_q$ transgene in cells of the osteoblast lineage exhibited severe osteopenia in cortical and trabecular bones. Osteoblast number, bone volume, and trabecular thickness were reduced in transgenic mice, but the osteoclasts were unaffected. Osteoblasts from transgenic mice showed impaired differentiation and matrix formation. In the presence of a protein kinase C inhibitor GF109203X, this impairment was not seen, indicating mediation by the protein kinase C pathway. We propose that continuous activation of the $G\alpha_q$ signal in osteoblasts plays a crucial, previously unrecognized role in bone formation.

G-proteins, heterotrimeric guanine nucleotide-binding proteins that interact with the cytoplasmic domains of membrane-embedded receptors, transduce extracellular signals that affect many biological actions. Although pathways regulated by G-proteins remain to be elucidated in bone cells, activation of several G-protein-coupled receptors (GPCR),[2] including those for parathyroid hormone (PTH) and prostaglandins, affects bone formation (1). A great deal has been learned concerning G-protein function in the skeleton and elsewhere from naturally occurring human mutations in $G\alpha_s$ (2). Somatic $G\alpha_s$ mutations of key residues required to terminate GTPase are present in various endocrine tumors and fibrous dysplasia of bone, and in a more widespread distribution in patients with McCune-Albright syndrome, which is characterized by localized bone lesions termed polyostotic fibrous dysplasia, cafe-au-lait pigmentation of the skin, and autonomous hyperfunction of multiple endocrine organs. Substitution of Arg-201 of $G\alpha_s$ with either Cys or His causes the inhibition of the intrinsic GTPase activity, resulting in prolonged stimulation of adenylate cyclase and increased cAMP production in the affected tissues (3–5). Heterozygous inactivating $G\alpha_s$ mutations lead to Albright hereditary osteodystrophy, a congenital syndrome in which patients develop obesity, short stature, brachydactyly, subcutaneous ossifications, and neurobehavioral deficits (5, 6). $G\alpha_s$ is imprinted in a tissue-specific manner. Maternally inherited mutations lead to pseudohypoparathyroidism type 1A, and paternally inherited mutations lead to Albright hereditary osteodystrophy alone, and pseudohypoparathyroidism type 1B is almost always associated with a *GNAS* imprinting defect in which both alleles have a paternal specific imprinting pattern on both parental alleles. Moreover, mice with osteoblast-specific $G\alpha_s$ deficiency was generated recently, and this deficiency led to a defect in the formation of the primary spongiosa with reduced immature osteoid and thickened cortical bone with narrowing of the bone marrow cavity, implying a strong involvement of the $G\alpha_s$ signal in bone development (7). On the other hand, $G\alpha_q$ mutations have not been reported in human disease, perhaps because the functional redundancy of $G\alpha_q$ and $G\alpha_{11}$ would compensate for a loss-of-function mutation, and little is known regarding the $G\alpha_q$ signaling role in bone cells. Although PKA is reported to be linked to many changes in gene expression directed by GPCRs in osteoblasts (8), the potential roles of PKC in osteoblast proliferation and differentiation are poorly understood.

Our purpose here is to examine the role of the $G\alpha_q$-mediated PKC signal in osteoblasts *in vitro* and *in vivo*. We first studied the effect of constitutively active $G\alpha_q$ signaling on osteoblast differentiation by overexpressing the epitope-tagged (HA), constitutively active mutant (Q209L) of the $G\alpha_q$ subunit (HA-CA-$G\alpha_q$) (9) *in vitro* in osteoblastic cells. Next, to study the role of $G\alpha_q$ signaling *in vivo*, we produced mice that expressed a transgene encoding HA-CA-$G\alpha_q$ under the control of 2.3-kb type I collagen α1 chain (*Col.1*) promoter (10), thus limiting expression nearly exclusively to osteoblasts. This study demonstrated that $G\alpha_q$-mediated activation of PKC in osteoblasts plays a crucial role in bone formation by inhibiting the differentiation of osteoblasts.

EXPERIMENTAL PROCEDURES

Cell Culture—Mouse osteoblastic MC3T3-E1 cells were cultured in α-minimal essential medium (αMEM), 10% FBS, and 1% penicillin/streptomycin (Invitrogen). In experiments

* This work was supported by National Institutes of Health Grants DK11794 and DK47034 (to G. V. S.). The costs of publication of this article were defrayed in part by the payment of page charges. This article must therefore be hereby marked "*advertisement*" in accordance with 18 U.S.C. Section 1734 solely to indicate this fact.

[1] To whom correspondence should be addressed: Sensory & Motor System Medicine, Faculty of Medicine, University of Tokyo, Hongo 7-3-1, Bunkyo, Tokyo 113-8655, Japan. Tel.: 81-33815-5411 (Ext. 30473); Fax: 81-33818-4082; E-mail: kawaguchi-ort@h.u-tokyo.ac.jp.

[2] The abbreviations used are: GPCR, G-protein-coupled receptor; ALP, alkaline phosphatase; αMEM, α-modified MEM; BMD, bone mineral density; CA, constitutively active; Col.1, type I collagen α1 chain; G3PDH, glyceraldehyde-3-phosphate dehydrogenase; HA, hemagglutinin; OCN, osteocalcin; PBS, phosphate-buffered saline; PKC, protein kinase C; PTH, parathyroid hormone; TG, transgenic-type; WT, wild-type; RANKL, receptor activator of NF-κB ligand; RT, reverse transcription; PKA, cAMP-dependent protein kinase; FBS, fetal bovine serum.

assessing differentiation, medium was supplemented with β-glycerophosphate and ascorbic acid (Sigma). Fresh medium was added twice per week.

Stable Transfection—MC3T3-E1 cells were plated at a density of 3×10^3 cells/cm^2. After 24 h, these cells were transfected with the HA-tagged, constitutively active $G\alpha_q$ (MC3T3-E1-$G\alpha_q$) cloned into pcDNA3.1 (Invitrogen) or with the empty vector (MC3T3-E1-EV) using calcium phosphate precipitation. Replacing amino acids 125–130 in $G\alpha_q$ with part of the HA epitope does not interfere with its function (9). After 24 h, and every 48 h thereafter, the medium was replaced with fresh medium containing 200 μg/ml of hygromycin. By limiting dilution, more than 200 clones of MC3T3-E1-$G\alpha_q$ and more than 50 clones of MC3T3-E1-EV were established; clones were selected for further study based on measurement of total inositol phosphates as described previously (11).

Alkaline Phosphatase (ALP) Activity—MC3T3-E1-EV and MC3T3-E1-$G\alpha_q$ clones were plated at a density of 2×10^4 cells/cm^2 and cultured for periods ranging from 3 to 21 days. At various intervals, the ALP activity in cell lysates was assessed in assay buffer (50 mM Tris-HCl (pH 7.6), and 0.1% Triton X-100) containing 1.5 M 2-amino-2-methyl-1-propanol for 30 min at 37 °C using *p*-nitrophenyl phosphate as a substrate. The release of *p*-nitrophenol was monitored by measuring absorbance at 405 nm.

Generation of Transgenic (TG) Mice—A DNA fragment containing the 2.3-kb osteoblast-specific promoter region of the mouse *Col.1* was inserted into KpnI/XbaI site of the intermediate vector to generate the final expression construct. The ends of this fragment were made blunt with Klenow polymerase and ligated to a blunt-ended BamHI site in the pcDNAI plasmid that contained a 1.1-kb cDNA fragment that encoded the entire coding sequence for HA epitope-tagged, constitutively active G_q protein α subunit (HA-$G\alpha_q$) (9). Restriction endonuclease digestions and nucleotide sequence analysis confirmed the correct orientation of the construct. The fragment from the final construct, including the 2.3-kb *Col.1* promoter and HA-$G\alpha_q$, was purified according to standard techniques and injected into the pronuclei of fertilized eggs from FVB/N mice by the Massachusetts General Hospital Transgenic Facility (Boston). Founder mice of the FVB/N strain were mated with WT mice to establish individual transgenic lines. The cDNA encoding for mouse HA-$G\alpha_q$ (Q209L) was provided by E. J. Neer (Brigham and Women's Hospital and Harvard Medical School, Boston). The 2.3-kb osteoblast-specific promoter region for the mouse *Col.1* was provided by B. de Crombrugghe (The University of Texas, Houston). All mice were maintained according to the protocol approved by the institutional animal care committee.

Screening for TG Mice by the PCR—To screen for TG animals, we performed PCR using *Taq*DNA polymerase (Promega Corp., Madison, WI) and 100–200 ng of DNA prepared from mice tails using the DNeasy tissue kit (Qiagen Inc., Valencia, CA) according to the manufacturer's directions. The PCR was performed for 40 cycles using the primer pairs encompassing nucleotides 397–421 (GACGTCCCCGACTACGCGGCAATAA) of the HA-$G\alpha_q$ cDNA, including an HA tag, and nucleotides 579–599 (TATTCGATGATCCCTGTAGTG) of the $G\alpha_q$ cDNA with the thermal cycle set at 94 °C for 30 s, 50 °C for 30 s, and 72 °C for 2 min.

Transgene mRNA Expression—To investigate tissue-specific expression of the transgene, we reverse-transcribed total cellular RNA from mouse tissues and then performed PCR (RT-PCR). The reverse transcription reaction was performed with Superscript reverse transcriptase (Invitrogen) and oligo(dT) primers using 2 μg of total cellular RNA prepared with the TRIzol reagent (Invitrogen) according to the manufacturer's directions. Prior to the PCR, total cellular RNA was treated with DNase (Invitrogen) according to the manufacturer's directions. The reverse transcription reaction was performed using Superscript reverse transcriptase (Invitrogen) and oligo(dT) primers according to the manufacturer's directions. PCR was performed for 30 cycles using *Taq*DNA polymerase (Promega) and primer pairs encompassing nucleotides 397–421 (GACGTCCCCGACTACGCGGCAATAA) of the HA-$G\alpha_q$ cDNA, including an HA tag and nucleotides 579–599 (TATTCGATGATCCCTGTAGTG) of the $G\alpha_q$ cDNA with the thermal cycler set at 94 °C for 30 s, 50 °C for 30 s, and 72 °C for 2 min. Control PCRs were performed for 30 cycles using glyceraldehyde-3-phosphate dehydrogenase (G3PDH), 5′-CATGTAGGCCATGAGGTCCACCAC-3′ and 5′-TGAAGGTCGGTGTGAACGGATTTGGC-3′, with the thermal cycler set at 94 °C for 30 s, 58 °C for 30 s, and 72 °C for 2 min. PCR products were separated on 1.2% agarose gels and visualized by staining with ethidium bromide.

Serology—Serum was collected at 1 month of age for ionized calcium. Ionized calcium was measured by the 634 Ca^{2+}/pH analyzer (Ciba-Corning Diagnostics Corp., Medfield, MA). Intact immunoreactive PTH was measured in duplicate using enzyme-linked immunosorbent assay (Immutopics Inc., San Clemente, CA), which uses two affinity-purified polyclonal antibodies raised to peptides common to rat and mouse PTH.

Analysis of Bone Morphology—Bone radiographs of the excised femora and tibiae from 8-week-old WT and TG mice were taken with a soft x-ray apparatus (type SRO-M50; Sofron, Tokyo, Japan). Three-dimensional computed tomography scans were reconstructed using a composite x-ray analyzing system (NS-ELEX, Tokyo, Japan). Bone mineral density (BMD) was measured by single energy x-ray absorptiometry utilizing a bone mineral analyzer (DCS-600R, Aloka Co., Tokyo, Japan). For histological analyses, mice were killed at birth, 2, 4, and 8 weeks of age, and tibial and calvarial bone sections (5 μm) were fixed in 4% paraformaldehyde, 0.1 M PBS, decalcified by 10% EDTA, embedded in paraffin, and stained with hematoxylin and eosin. Collagen fiber deposition was assessed under polarized light in tibial and calvarial bone sections (5 μm) that had been fixed in 4% paraformaldehyde, 0.1 M PBS, decalcified by 10% EDTA, embedded in paraffin, and stained with hematoxylin and eosin. For the assessment of dynamic histomorphometric indices, mice were injected twice with calcein at a dose of 0.16 mg/10 g body weight and analyzed at 4 or 8 weeks of age. The 4-week group received dual injections 6 and 3 days before sacrifice, and the 8-week group received them 10 and 3 days before sacrifice. Long bones were fixed with ethanol, and the undecalcified bones were embedded in glycolmethacrylate. Three-μm longitudinal sections from the proximal tibiae and

20-μm cross-sections from mid-diaphyses of femora were stained with toluidine blue and analyzed using a semi-automated system (Osteoplan II; Zeiss). Parameters for trabecular bone were measured in an area 1.2 mm in length from 0.1 mm below the growth plate at the proximal metaphysis of the tibiae. Parameters for cortical bone were measured at the midshaft of the tibiae.

In Situ Hybridization—In situ hybridizations were performed as described (12) using complementary ^{35}S-labeled riboprobes (complementary RNAs and cRNAs) transcribed from the plasmids encoding human Col.1 and mouse osteocalcin.

Ex Vivo Cell Cultures—Osteoblastic cells were isolated from calvariae of neonatal (1–2 days old) WT and TG mice as described previously (13). Calvariae were digested at 37 °C for 10 min in an enzyme solution containing 0.1% collagenase and 0.2% dispase in αMEM for five cycles, and cells isolated in the last four digestions were combined as osteoblastic cells. Bone marrow cells were collected from long bones of 8-week-old mice and were plated at a density of 10^6 cells on a 6-multiwell plate. Osteoblastic cells and marrow cells were cultured in αMEM containing 10% FBS, 50 mg/ml ascorbic acid, and 1% penicillin/streptomycin. To assess mineralization, medium was supplemented with 10 nM β-glycerophosphate (Sigma). Fresh medium was added twice per week. To quantify cell proliferation, primary osteoblastic cells were inoculated at a density of 1×10^4 cells/well in a 24-multiwell plate, and cultured in the same medium for 3, 6, 9, and 12 days. [^{3}H]Thymidine (1 mCi/ml of medium) was added for the final 3 h of incubation after 24 h of culture, and incorporation was measured. To measure ALP activity, primary osteoblastic cells were inoculated at a density of 2×10^4 cells/well in a 24-multiwell plate and cultured in the same medium in the absence or presence of PKC inhibitor, GF109203X (100 ng/ml) (Calbiochem-Novabiochem). After 14 days of culture, the cells were washed with PBS and sonicated in 10 mM Tris-HCl buffer (pH 8.0) containing 1 mM $MgCl_2$ and 0.5% Triton X-100. ALP activity in the lysate was measured by the hydrolysis of *p*-nitrophenyl phosphate to *p*-nitrophenol. The protein content was determined using BCA protein assay reagent (Pierce). For measurement of mineralized matrix formation and calcium deposition, primary osteoblastic cells were plated at a density of 2×10^4 cells/cm^2 and cultured for 28 days. The formation of mineralized matrix nodules was assessed by Alizarin red staining, and the Alizarin red dye was eluted and measured spectrophotometrically to quantify calcium.

Northern Blotting and RT-PCR—For Northern blot analysis, osteoblasts were incubated at a density of 2×10^4 cells per dish in 100-mm dishes and cultured in αMEM containing 10% FBS with 50 mg/ml ascorbic acid. Total RNA was extracted using a TRIzol kit (Invitrogen). Ten μg of total RNA was electrophoresed in 1.2% agarose-formaldehyde gels and transferred onto nylon membrane filters (Hybond-N; Amersham Biosciences). cDNAs were labeled with [^{32}P]dCTP by a random primed labeling kit (Amersham Biosciences) according to the manufacturer's protocol. The membranes were hybridized for 2 h at 68 °C with cDNA probes for mouse Runx2, Col.1, osteocalcin, RANKL, and osteoprotegerin, prepared from the plasmids described previously. The membranes were then washed and analyzed by a Cyclone PhosphorImager (Hewlett-Packard, Palo Alto, CA). Control hybridization with G3PDH verified that equal amounts of RNA had been loaded. Semi-quantitative RT-PCR was performed within the exponential amplification range to assess for expression of the transgene. Total mRNA (1 μg) was reverse-transcribed, and PCR was performed using specific primer pairs for transgene and G3PDH described above.

Statistical Analysis—All data are expressed as means ± S.E. Means of groups were compared by analysis of variance, and significance of differences was determined by post hoc testing using the Bonferroni method.

RESULTS

Constitutive Signaling by $G\alpha_q$ Inhibits Differentiation of MC3T3-E1 Cells—We initially evaluated whether expression of the constitutively active $G\alpha_q$ subunit affected proliferation and/or differentiation of MC3T3-E1 cells. MC3T3-E1 cells were chosen because they are "pre-osteoblasts"; specifically, they differentiate into mature osteoblasts and form mineralized nodules under a defined culture condition.

We have established more than 200 MC3T3-E1 cell clones in total that stably overexpressed $G\alpha_q$, and the range of increases in the protein level was 1.4–5.0-fold. Among them, three clones ($G\alpha_q$ clones -29, -135, and -155) with ~2-fold higher $G\alpha_q$ protein expression were selected, because they also caused higher levels of PKC activity determined by the total inositol phosphate uptake than those of three control clones transfected with the empty vector (EV-1, -2, and -3) (Fig. 1*A*). Interestingly, most of the clones that expressed more than 3-fold of the $G\alpha_q$ protein neither showed higher uptake of total inositol phosphate nor did they grow well, resulting in abnormal morphological changes of cell shape (data not shown).

Proliferation of the selected three MC3T3-E1-$G\alpha_q$ and the MC3T3-E1-EV cell lines was indistinguishable within each group and between groups, as assessed by counting cells at regular intervals; cell morphology also was not notably different (data not shown). However, the differentiation of the MC3T3-E1-$G\alpha_q$ cells determined by ALP activity was significantly lower during 21 days of culture (Fig. 1*B*), and a mineralized bone nodule formation determined by Alizarin red staining was also suppressed after 28 days (Fig. 1*C*), as compared with MC3T3-E1-EV clones. Additionally, mRNA levels of osteoblast differentiation markers Runx2, Col.1, and osteocalcin were lower in MC3T3-E1-$G\alpha_q$ clones than in MC3T3-E1-EV clones (Fig. 1*D*). Because the differences were more conspicuous at the earlier days than at 14 days, the $G\alpha_q$-mediated signaling was likely to affect not only matrix formation by mature osteoblasts but also early stages of osteoblast differentiation.

Generation of Mice Overexpressing Constitutively Active $G\alpha_q$ in Osteoblastic Cells—We then generated mice that express the constitutively active mutant of $G\alpha_q$ in cells of the osteoblast lineage, by controlling expression using the 2.3-kb proximal promoter of *Col.1* gene (Fig. 2*A*). Independent transgenic lines were established from two male founders, and indistinguishable results were obtained from analyses of the progeny from both founder lines. Bone-specific expression of the transgene was confirmed by reverse transcription of total RNA, after it had been extracted from numerous tissues, followed by PCR using HA epitope-specific sense and $G\alpha_q$ antisense primers

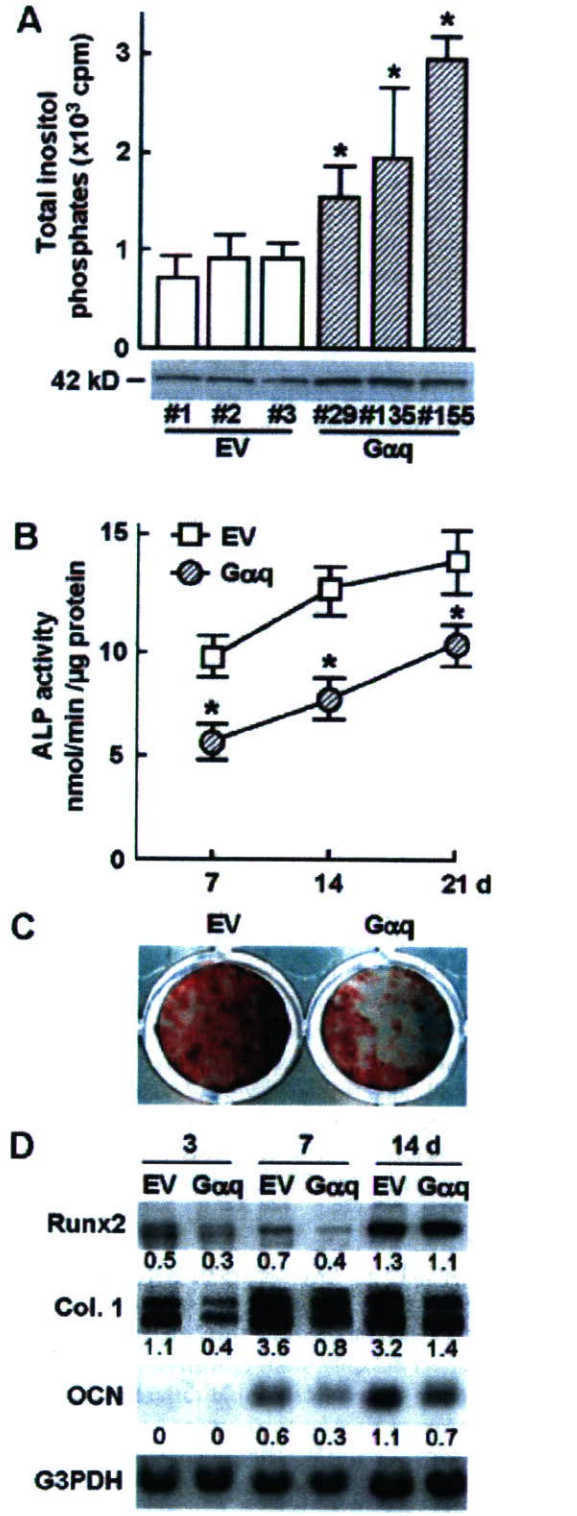

FIGURE 1. **Overexpression of constitutively active $G\alpha_q$ in MC3T3-E1 cells.** *A*, total inositol phosphates and Western blotting using an anti-$G\alpha_q$ antibody in selected stable MC3T3-E1 cell lines that express either constitutively active $G\alpha_q$ (*-29, -135,* and *-155*) or empty vector (*EV-1, -2,* and *-3*). *B*, ALP activity of $G\alpha_q$ (*-155*) and MC3T3-E1-EV (*-1*) at 7, 14, and 21 days of culture. *C*, Alizarin red staining of MC3T3-E1-$G\alpha_q$ (*-155*) and MC3T3-E1-EV (*-1*) cultured for 28 days. *D*, Runx2, type I collagen (Col.1), and OCN mRNA levels determined by Northern blotting of MC3T3-E1-$G\alpha_q$ (*-155*) and MC3T3-E1-EV (*-1*) cells. Control hybridization with a G3PDH probe verified the amount of RNA loaded. Blots were quantified using densitometry and indicated as ratios normalized to those of respective G3PDH.

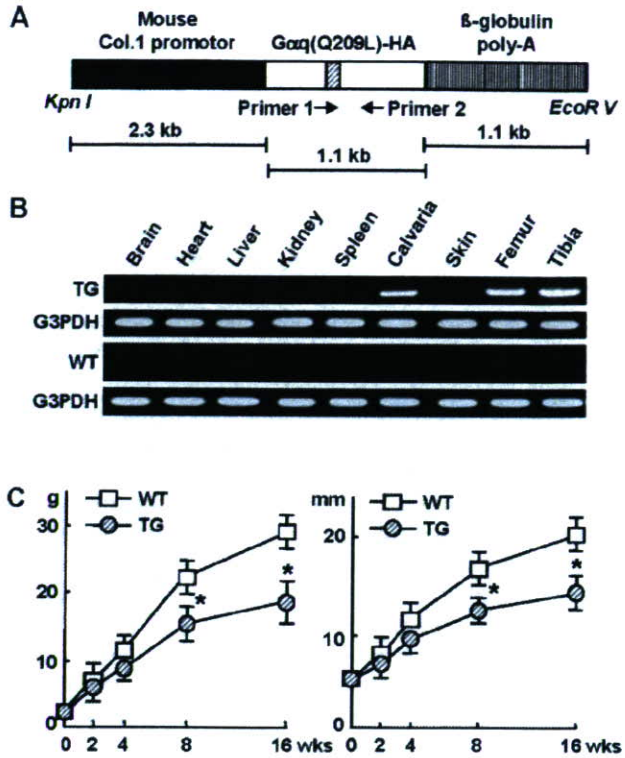

FIGURE 2. **Transgene construct and its expression.** *A*, schematic representation of mouse *Col.1* promoter-constitutively active $G\alpha_q$ transgene. *Slashed box* indicates the region of the entire coding of HA tag. The location of forward and reverse primers for RT-PCR is indicated by the *arrows*. *B*, RT-PCR product of the predicted size was detected only in total RNA extracted from bones of TG mice. The transgene was not detected in other tissues from TG mice nor in any tissues from the WT littermates. Control PCRs revealed a PCR product of the appropriate size in all tissues using the G3PDH primers. *C*, body weight (*left*) and tibial length (*right*) of WT and TG mice at indicated ages. Data are expressed as means (*symbols*) ± S.E. (*error bars*) for 10 mice/group/time. *, $p < 0.01$ *versus* WT mice.

(Fig. 2*B*). A PCR product of the appropriate size was detected in bone extracts from TG mice, but none was detected either in extracts from other tissues from TG mice or any tissues from WT littermates (Fig. 2*B*).

At birth, TG mice appeared normal, and their body weights and bone lengths were indistinguishable from WT littermates. Both males and females of the two transgenic lines showed qualitatively similar skeletal changes at all stages of postnatal development; however, the TG mice were smaller and had shorter limbs than WT littermates at 8 weeks and thereafter (Fig. 2*C*). Among 30 TG mice, tibial fracture was observed in nine mice as early as 2 weeks of age, although none in WT, indicating that the skeleton of TG mice was fragile. Craniofacial development and tooth eruption were normal in TG mice.

Blood-ionized calcium concentration and intact PTH levels were comparable between WT and TG mice at 4 weeks of age (ionized Ca^{2+} (mM): WT mice, 1.26 ± 0.02, $n = 10$; TG mice, 1.28 ± 0.03, $n = 10$, $p > 0.1$ *versus* WT mice and PTH (pg/ml); WT mice, 35.3 ± 3.3, $n = 10$; TG mice, 34.2 ± 4.4, $n = 10$, $p > 0.1$ *versus* WT mice).

All data are expressed as means (*bars* and *symbols*) ± S.E. (*error bars*) of three independent experiments. *, $p < 0.01$ *versus* MC3T3-E1-EV. Similar results were obtained in other cell lines ($G\alpha_q$ *29* or *135 versus EV2* or *EV3*).

Radiographic and Histological Skeletal Analyses—Long bones of WT and TG mice at birth were grossly indistinguishable as were the radiological and histological analyses of the physis, epiphysis, and diaphysis (data not shown). Also, at all ages examined, no difference was apparent in height or morphology of growth plate cartilage. Plain x-ray of long bones showed that TG mice at 8 weeks were proportionally shorter than WT mice and showed severe osteopenia (Fig. 3*A*). Three-dimensional femoral computed tomography analyses demonstrated thinner cortices and fewer trabeculae in TG mice compared with WT littermates, indicating that both cortical and trabecular bone were affected (Fig. 3*A*). BMDs of the entire femur and tibia of TG mice were significantly lower than those of WT mice at 4 and 8 weeks of age (Fig. 3*B*).

By histological examination of the proximal tibiae, osteopenia began to be detected in TG mice at 2 weeks of age, which became evident at 4 weeks with decreases in both cortical thickness and trabecular number, as compared with WT littermates (Fig. 3*C*). In addition to being thinner, a polarized microscopic image of the TG cortical bone revealed that the extracellular matrix was more disorganized, suggesting a woven bone pattern, than the WT matrix with lamellar distribution. Marrow fibrosis that can sometimes accompany woven bone (14), however, was not detected in the marrow cavity of TG mice. The decreases in cortical and trabecular bone volumes were still evident without widening of osteoid seams at 8 weeks in TG mice, as shown in the toluidine blue staining (Fig. 3*C*). We further examined the *in vivo* expressions of Col.1 and osteocalcin by *in situ* hybridization at 2 weeks of age when osteopenia became detectable. The expressions were decreased in trabecular and cortical bones of TG mice (Fig. 3*D*).

Bone Histomorphometric Analyses—Bone histomorphometric measurements of trabecular bones from mice of 4 and 8 weeks of age showed that parameters of bone formation, bone volume (BV/TV), trabecular thickness (Tb.Th), osteoblast number (Ob.S/BS), and osteoid surface (OS/BS), were markedly reduced in TG mice at both ages, whereas parameters of bone resorption (number of mature osteoclasts (Oc.N/B.Pm), percentage of bone surface covered by mature osteoclasts (Oc.S/BS), percentage of eroded surface (ES/BS)) were not significantly different (Fig. 4*A*). Cortical thickness (Ct.Th) at the midshaft of tibiae was also decreased in TG mice at both ages.

Dynamic analyses of bone formation performed by double labeling with calcein at a 3-day interval in 4-week-old mice and a 7-day interval in 8-week-old mice in trabecular bone showed two widely spaced bands of calcein deposition in 4-week-old WT mice (Fig. 4*B*). In contrast, bone from TG mice showed only a single or two only narrowly separated lines. Trabecular dynamic histomorphometry was performed on longitudinal sections of 4- and 8-week-old bone. Compared with the WT littermates, TG mice had significantly lower bone formation and mineral apposition rates but similar mineralization lag time at both ages (Fig. 4*B*). No sex differences were apparent for these quantitative analyses. Our attempts at comparison of the apoptosis of osteoblasts and osteocytes in WT and TG mice showed no significant difference (data not shown).

Ex Vivo Analyses of Primary Osteoblasts—To further examine the cellular mechanism underlying the abnormalities in bone formation in TG mice, osteoblasts were isolated from neonatal calvariae of TG and WT mice, grown in culture and studied after two passages.

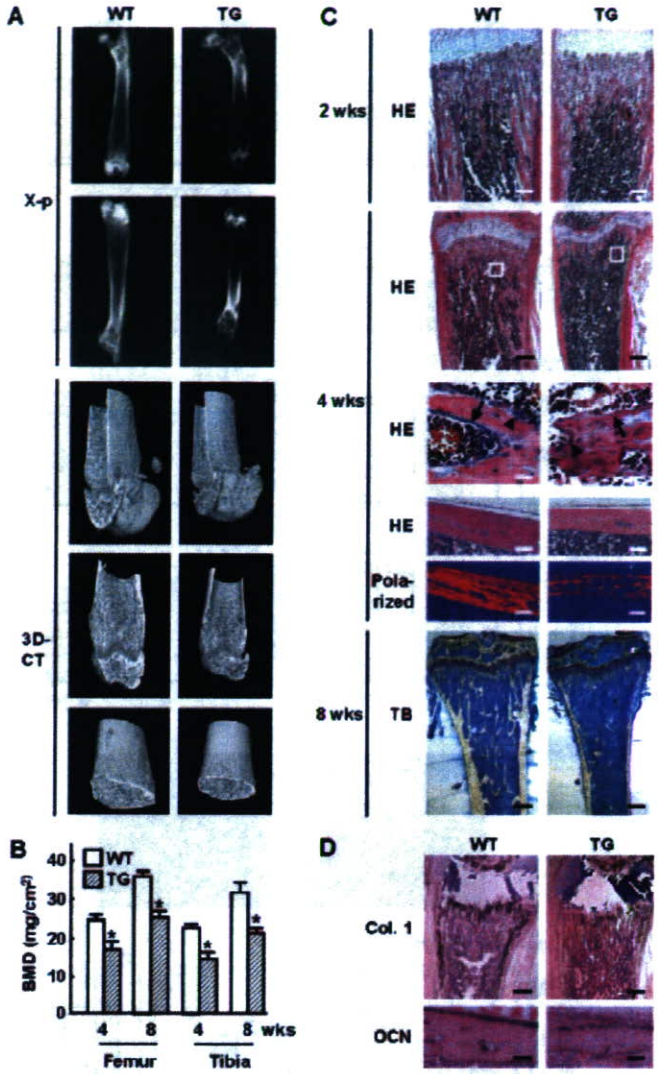

FIGURE 3. **Radiological and histological findings of the long bones in WT and TG mice littermates.** *A*, plain x-ray of whole femora and tibiae, and three-dimensional computed tomography reconstructed images of the distal femora of representative 8-week-old WT and TG male littermates. *B*, BMD of the femora and tibiae of WT and TG littermates at 4 and 8 weeks of age. Data are expressed as mean (*bars*) ± S.E. (*error bars*) for five mice/group/time. *, $p < 0.01$ *versus* WT mice. *C*, longitudinal decalcified sections through the proximal tibia of 2- or 4-week-old WT and TG mice and decalcified sections of cortical bone from tibial mid-diaphysis of 4-week-old WT and TG mice were stained with hematoxylin and eosin (*HE*; *scale bar*, 100 μm (proximal tibiae of 2-week-old mice), 200 μm (proximal tibiae of 4-week-old mice), and 20 μm (cortical bone)). *Inset boxes* indicate the region of the row below (*HE*; *scale bar*, 10 μm. *Arrows* and *arrowheads* indicate osteoblasts and osteoclasts, respectively.). Collagen fiber deposition was assessed under polarized microscopy in cortical bone sections (*scale bar*, 20 μm). Sections of undecalcified proximal tibia of 8-week-old WT and TG mice were stained by toluidine blue (*TB*; *scale bar*, 400 μm). Data of histomorphometric analyses are shown in Fig. 4. Sections shown are representative of those obtained from six mice in each group. *D*, *in situ* hybridization with the ^{35}S-labeled type I collagen (*Col.1*) and OCN cRNAs in sections of decalcified proximal tibia (*scale bar*, 200 μm) and tibial cortex (*scale bar*, 20 μm), respectively, from 2-week-old WT and TG mice. The bright field sections were counterstained with hematoxylin and eosin. Representative images were selected from 10 to 12 mice/genotype, which showed consistent results.

First, expression of the transgene was detected only in osteoblasts from TG lines, not in cells from WT littermates, by RT-

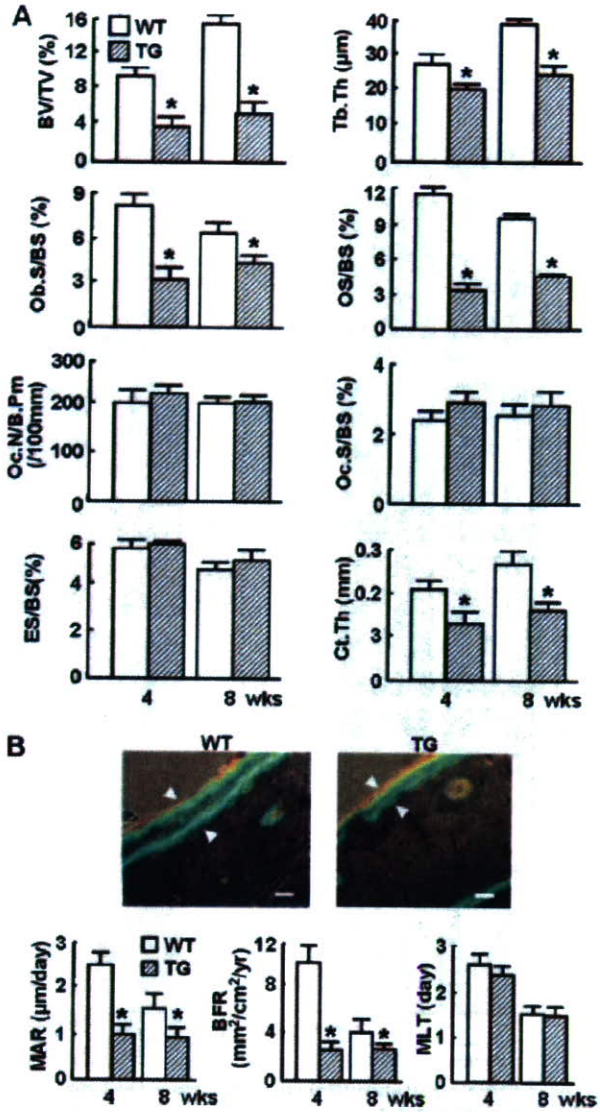

FIGURE 4. **Histomorphometric analyses of trabecular and cortical bones.** *A*, static parameters of trabecular bones from 0.1 to 1.2 mm below the growth plate of the proximal tibiae metaphysis were compared between 4- and 8-week-old WT and TG mice. *BV/TV*, trabecular bone volume as a percentage of total volume; *Tb.Th*, trabecular thickness; *Ob.S/BS*, percentage of the bone surface covered by cuboidal osteoblasts; *OS/BS*, percentage of the bone surface covered with osteoid; *Oc.N/B.Pm*, number of mature osteoclasts in 10 cm of the bone perimeter; *Oc.S/BS*, percentage of bone surface covered by mature osteoclasts; *ES/BS*, percentage of eroded surface. Cortical thickness (*Ct. Th*) was also compared at the midshaft of tibiae. *B*, dynamic parameters of bone formation in trabecular bone. Tibial mineralization fronts of 4-week-old WT and TG mice were imaged by fluorescent microscopy, after labeling with calcein at days 3 and 6 (*scale bar*, 50 μm), and longitudinal sections from proximal parts of tibiae of WT and TG mice at 4 and 8 weeks of age were used for measurement of mineral apposition rate (*MAR*), bone formation rate (*BFR*), and mineralization lag time (*MLT*). Data are expressed as means (*bars*) ± S.E. (*error bars*) for five mice/group/time. *, $p < 0.01$ *versus* WT mice.

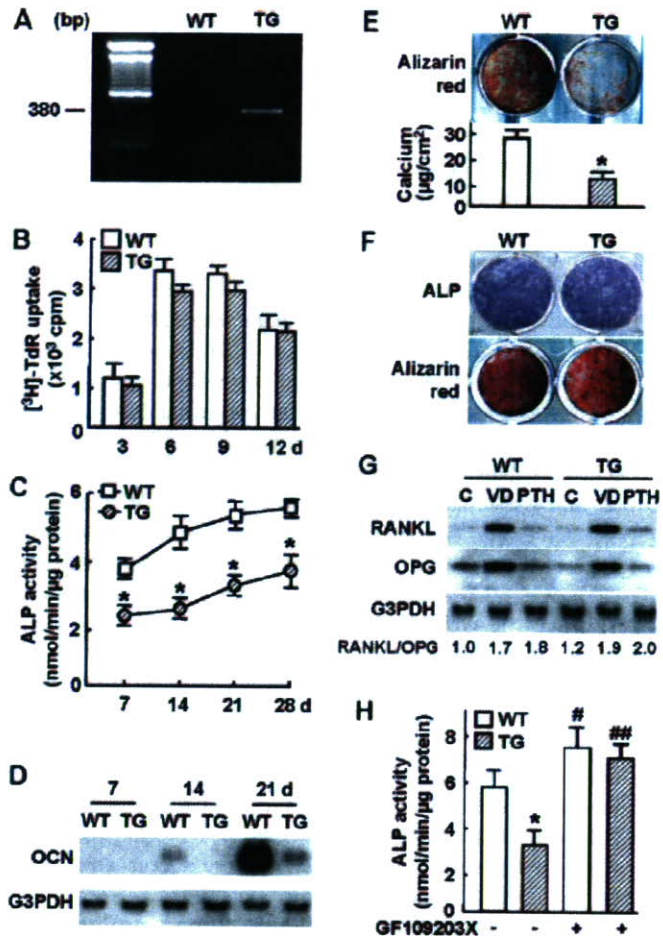

FIGURE 5. ***Ex vivo* analyses of cultured osteoblasts or bone marrow cells.** *A*, RT-PCR for the transgene using total RNA extracted from primary cultured osteoblasts from neonatal calvariae of WT or TG mice. *B*, time course of [³H]thymidine incorporation into calvarial osteoblasts. *C*, time course of ALP activity of calvarial osteoblasts. *D*, Northern blotting for OCN expression in calvarial osteoblasts. *E*, Alizarin red staining of calvarial osteoblasts cultured for 28 days (*top*) and quantification of matrix-bound calcium (*bottom*). *F*, ALP and Alizarin red stainings of bone marrow cells from 8-week-old WT or TG mice at 14 and 28 days of culture, respectively. *G*, Northern blotting for RANKL and osteoprotegerin (*OPG*) expressions in calvarial osteoblasts cultured with or without $1,25(OH)_2D_3$ (1 nM) (*VD*) or PTH (10 nM) for 7 days. Control hybridization with a G3PDH probe verified the amount of RNA loaded. Blots were quantified using densitometry, and relative RANKL/osteoprotegerin ratio was calculated after the density of each blot was normalized to that of the respective G3PDH. *H*, ALP activity of calvarial osteoblasts in the presence and absence of GF109203X (100 nM) at 14 days of culture. Data are expressed as means (*bars* and *symbols*) ± S.E. (*error bars*) of three independent experiments; each experimental condition was done in triplicate. *, $p < 0.01$ *versus* WT osteoblasts; #, $p < 0.05$ *versus* WT osteoblasts without GF109203X; ##, $p < 0.01$ *versus* TG osteoblasts without GF109203X.

PCR using transgene-specific primers (Fig. 5*A*). Proliferation rates of osteoblasts from TG and WT littermates were similar at 3, 6, 9, and 12 days in culture, when pulse-labeled with [³H]thymidine, confirming that the impaired bone formation in TG mice is not because of diminished proliferation (Fig. 5*B*).

Next, we assessed osteoblast maturation. Both ALP activity and osteocalcin expression were lower in TG osteoblasts than in WT (Fig. 5, *C* and *D*). Alizarin red staining and extracellular matrix-bound calcium levels were also severely decreased, confirming a decrease of matrix formation, in the TG osteoblast culture (Fig. 5*E*). Conversely, there was a slight suppression of ALP and Alizarin red staining in cultures of bone marrow cells from 8-week-old TG mice, indicating that marrow cells were less affected by $G\alpha_q$ activation than osteoblasts (Fig. 5*F*). RANKL and osteoprotegerin mRNA levels, and the RANKL/osteoprotegerin ratio were similar in WT and TG osteoblasts (Fig. 5*G*), consistent with the *in vivo* resorption parameters of histomorphometric analysis (Fig. 4*A*). When bisindolylmaleimide (GF109203X), a PKC inhibitor, was added to the cultures,

inhibition of ALP activity by $G\alpha_q$ overexpression was not seen (Fig. 5*H*), indicating that the impaired osteoblast differentiation by $G\alpha_q$ is at least partly mediated by the PKC pathway.

DISCUSSION

We have shown that mice with osteoblast-specific expression of a constitutively active $G\alpha_q$ transgene exhibited proportionate dwarfism that became apparent by the 2nd postnatal week, and it progressed at least until 8 weeks after birth. There was no unusual gestational or perinatal lethality, nor did the mice manifest an atypical life span. The phenotype was characterized by deficient intramembranous and endochondral bone, despite apparently normal growth-plate chondrogenesis, osteopenia, and skeletal fragility, manifested by nontraumatic long bone fractures. Histology revealed reduced thickness of cortical and trabecular bones, with a decrease in lamellar bone and an increase in immature bone. The rate of bone formation was decreased because of an inhibition of osteoblast differentiation, without an alteration in osteoblast proliferation. The decrease of mineralized matrix in the cultures of osteoblasts with higher $G\alpha_q$ expression (Fig. 1*C* and Fig. 5*E*) represents the cumulative consequence of impairment in osteoblast differentiation and matrix production rate during 28 days of cultures. However, the absence of widened osteoid seams *in vivo* indicates the lack of defect in the mineralization process. The fact that inhibitory effects of the $G\alpha_q$ overexpression on osteoblastic markers were more conspicuous at earlier days (Fig. 1*D*) also supports the suppression in the process of osteoblast differentiation rather than the later stages. In addition, treatment of TG osteoblasts *ex vivo* with the PKC inhibitor, GF109203X, confirmed and extended these observations by showing that the impaired differentiation in TG osteoblasts was because of the continuous activation of PKC. Therefore, PKC activation by $G\alpha_q$ may impair osteoblast differentiation, causing the reduced bone growth and bone formation.

Most previous data suggested that regulation of osteoblast differentiation by GPCR was mainly mediated via cAMP/PKA signaling (15), and little attention has been given to how $G\alpha_q$-mediated signaling affects bone formation (16, 17). *In vitro*, continued treatment of calvariae or osteoblastic cells with PTH has been shown to inhibit type I collagen expression and to increase osteocalcin expression largely via cAMP-dependent pathways (18, 19). Our data, showing suppression of osteoblast differentiation by continuous activation of $G\alpha_q$-undetectable expression of osteocalcin and impaired mineralization, may be the first to highlight a crucial inhibitory signaling role(s) for $G\alpha_q$/PKC in bone formation.

Cortical bone of TG mice was composed mainly of immature bone just like the woven bone in which the extracellular matrix ran in irregular directions and instead of the mature lamellar bone seen in the WT bone. Typically, woven bone is formed in pathological conditions like osteosarcoma and fracture callus, in which the bone turnover rate is accelerated (20). The present histomorphometric analysis of the TG bone, however, showed that bone formation was decreased and bone resorption was unaffected (Fig. 4). In addition, although $G\alpha_q$ signaling is known to be involved in the regulation of RANKL and osteoprotegerin (21), none of the expression levels or the ratio was changed in cultured TG osteoblasts (Fig. 5*G*). A recent work by Komori and co-workers (22) showed that transgenic mice that overexpressed Runx2 in osteoblasts exhibited osteopenia with woven bone, which was caused by the maturational suppression of osteoblasts at a late stage. Their work supports our finding that inhibition of osteoblast differentiation could lead to woven bone formation, although the impairment stage of differentiation was somewhat earlier in our TG mice than the Runx2 transgenic mice. Further studies will elucidate the mechanism underlying the organization of extracellular matrix regulated by osteoblast differentiation.

To date, no human diseases have been attributed to mutations in $G\alpha_q$. The lack of syndromes because of loss-of-function mutations are readily understood because of the redundant functionality of $G\alpha_q$ and $G\alpha_{11}$, making it necessary to have appropriate, simultaneous mutations in both genes. The absence of a syndrome because of a dominant-acting mutation is less apparent. If widespread in many tissues, perhaps it is lethal, as the cardiac overexpression of $G\alpha_q$ leads to hypertrophy and dilated cardiomyopathy with a short life span (23–25). Wettschureck *et al.* (26) recently reported that mice with parathyroid-specific double knock-out of $G\alpha_q$ and $G\alpha_{11}$ exhibited a phenotype resembling germ line knock-out of the extracellular Ca^{2+}-sensing receptor: severe hypercalcemia, hyperparathyroidism, hypocalciuria, retarded growth, and early postnatal death. Similarly, by using cre/lox technology, we are now generating double knock-out mice with osteoblast-specific ablation of $G\alpha_q$ and $G\alpha_{11}$, to learn more about the loss-of-function of $G\alpha_{q/11}$ in osteoblasts.

Classical teaching was that there was a linear relationship between the volume of hypertrophic chondrocytes and the rate of longitudinal bone growth and that limb-shortening defects were because of defects in the growth plate (27–30). Studies from Karsenty and co-workers (31) have challenged this paradigm. They first showed that ganciclovir ablation of osteoblasts in mice expressing the herpes simplex virus thymidine kinase gene under control of the osteocalcin promoter showed dwarfism with severely reduced longitudinal bone growth (31). Then they showed that overexpression of the Runx2 DNA binding domain, without the transcriptional activating domain, resulted in shortening of long bones and impaired bone formation (32). In addition, Pantschenko *et al.* (33) reported that overexpression of Bcl-2, an important regulator of apoptosis, in osteoblasts also resulted in shortening of long bones and an inhibition of bone loss with age. As with our mice, neither of these models had apparent chondrocyte defects in the growth plate. Although we cannot, of course, exclude expression of transgene at the growth plates at levels we could not detect, longitudinal bone growth might be determined by the deposition of bone matrix and/or bone formation, in addition to the chondrocyte proliferation and hypertrophy in the growth plates.

In conclusion, the present study demonstrated that $G\alpha_q$-mediated activation of PKC suppressed osteoblast differentiation, but not proliferation, *in vivo* and *in vitro*. Together, the effects on these phenomena led to decreased bone formation and pointed to a crucial, novel role for $G\alpha_q$/PKC signaling in osteoblast biology. We predict that a human syndrome(s) in which

bone formation is impaired, but as yet not reported, will be due to dominant-acting mutation(s) of $G\alpha_q$. Because PTH signals through $G\alpha_q$/PKC as well as $G\alpha_s$/PKA (34), further work to sort out the PTH signaling pathways in bone cells may reveal a potential pharmacological target for treatment of osteoporosis and other bone-loss states.

Acknowledgment—We thank the hard tissue research team at Kureha Chemical Co., Ltd. for technical assistance.

REFERENCES

1. Dohlman, H. G., Thorner, J., Caron, M. G., and Lefkowitz, R. J. (1991) *Annu. Rev. Biochem.* **60,** 653–688
2. Spiegel, A. M. (1997) *Horm. Res.* **47,** 89–96
3. Spiegel, A. M., Weinstein, L. S., and Shenker, A. (1992) *J. Clin. Investig.* **92,** 1119–1125
4. Weinstein, L. S., Shenker, A., Gejman, P. V., Merino, M. J., Friedman, E., and Spiegel, A. M. (1991) *N. Engl. J. Med.* **325,** 1688–1695
5. Weinstein, L. S., Yu, S., Warner, D. R., and Liu, J. (2001) *Endocr. Rev.* **22,** 675–705
6. Patten, J. L., Johns, D. R., Valle, D., Eil, C., Gruppuso, P. A., Steele, G., Smallwood, P. M., and Levine, M. A. (1990) *N. Engl. J. Med.* **322,** 1412–1419
7. Sakamoto, A., Chen, M., Nakamura, T., Xie, T., Karsenty, G., and Weinstein, L. S. (2005) *J. Biol. Chem.* **280,** 21369–21375
8. Quarles, L. D., and Siddhanti, S. R. (1996) *J. Bone Miner. Res.* **11,** 1375–1383
9. Wu, D. Q., Lee, C. H., Rhee, S. G., and Simon, M. I. (1992) *J. Biol. Chem.* **267,** 1811–1817
10. Rossert, J., Eberspaecher, H., and Crombrugghe, B. D. (1995) *J. Cell Biol.* **129,** 1421–1432
11. Iida-Klein, A., Guo, J., Xie, L. Y., Juppner, H., Potts, J. T., Kronenberg, H. M., Bringhurst, F. R., Abou-Samra, A. B., and Segre, G. V. (1995) *J. Biol. Chem.* **270,** 8458–8465
12. Calvi, L. M., Sims, N. A., Hunzelman, J. L., Knight, M. C., Giovannetti, A., Saxton, J. M., Kronenberg, H. M., Baron, R., and Schipani, E. (2001) *J. Clin. Investig.* **107,** 277–286
13. Ogata, N., Chikazu, D., Kubota, N., Terauchi, Y., Tobe, K., Azuma, Y., Ohta, T., Kadowaki, T., Nakamura, K., and Kawaguchi, H. (2000) *J. Clin. Investig.* **105,** 935–943
14. Weinstein, L. S. in *Principles of Bone Biology* (Bilezikian, J., Raisz, L., and Rodan, G., eds), 2nd Ed., pp. 877–888, Academic Press, San Diego
15. Bowler, W. B., Gallagher, J. A., and Bilbe, G. (1998) *Front. Biosci.* **3,** 769–780
16. Swarthout, J. T., Doggett, T. A., Lemker, J. L., and Partridge, N. C. (2001) *J. Biol. Chem.* **276,** 7586–7592
17. Kim, H. J., Kim, J. H., Bae, S. C., Choi, J. Y., Kim, H. J., and Ryoo, H. M. (2003) *J. Biol. Chem.* **278,** 319–326
18. Partridge, N. C., Dickson, C. A., Kopp, K., Teitelbaum, S. L., Crouch, E. C., and Kahn, C. (1989) *Mol. Endocrinol.* **3,** 232–239
19. Swarthout, J. T., D'Alonzo, R. C., Selvamurugan, N., and Partridge, N. C. (2002) *Gene (Amst.)* **282,** 1–17
20. Monier-Faugere, M. C. (1998) in *Metabolic Bone Disease* (Avioli, L. V., and Krane, S. M., eds) 3rd Ed., pp. 230–240, Academic Press, San Diego
21. Kondo, H., Guo, J., and Bringhurst, F. R. (2002) *J. Bone Miner. Res.* **17,** 1667–1679
22. Liu, W., Toyosawa, S., Furuichi, T., Kanatani, N., Yoshida, C., Liu, Y., Himeno, M., Narai, S., Yamaguchi, A., and Komori, T. (2001) *J. Cell Biol.* **155,** 157–166
23. Offermanns, S., Toombs, C. F., Hu, Y. H., and Simon, M. I. (1997) *Nature* **389,** 183–186
24. Mende, U., Kagen, A., Cohen, A., Aramburu, J., Schoen, F. J., and Neer, E. J. (1998) *Proc. Natl. Acad. Sci. U. S. A.* **95,** 13893–13898
25. Wettschureck, N., Rutten, H., Zywietz, A., Gehring, D., Wilkie, T. M., Chen, J., Chien, K. R., and Offermanns, S. (2001) *Nat. Med.* **7,** 1236–1240
26. Wettschureck, N., Lee, E., Libutti, S. K., Offermanns, S., Robey, P. G., and Spiegel, A. M. (2007) *Mol. Endocrinol.* **21,** 274–280
27. Breur, G. J., VanEnkevort, B. A., Farnum, C. E., and Wilsman, N. J. (1991) *J. Orthop. Res.* **9,** 348–359
28. Breur, G. J., Turgai, J., Vanenkevort, B. A., Farnum, C. E., and Wilsman, N. J. (1994) *Anat. Rec.* **239,** 255–268
29. Kember, N. F. (1978) *Cell Tissue Kinet.* **11,** 477–485
30. Kember, N. F. (1979) *J. Theor. Biol.* **78,** 365–374
31. Corral, D. A., Amlling, M., Priemel, M., Loyer, E., Fuchs, S., Ducy, P., Baron, R., and Karsenty, G. (1998) *Proc. Natl. Acad. Sci. U. S. A.* **95,** 13835–13840
32. Ducy, P., Starbuck, M., Priemel, M., Shen, J., Pinero, G., Geoffroy, V., Amling, M., and Karsenty, G. (1999) *Genes Dev.* **13,** 1025–1036
33. Pantschenko, A. G., Zhang, W., Nahounou, M., McCarthy, M. B., Stover, M. L., Lichtler, A. C., Clark, S. H., and Gronowicz, G. A. (2005) *J. Bone Miner. Res.* **20,** 1414–1429
34. Lanske, B., and Kovacs, C. S. (1998) *Recent Prog. Horm. Res.* **53,** 283–301

Osteoporos Int (2007) 18:1033–1046
DOI 10.1007/s00198-007-0343-y

ORIGINAL ARTICLE

The use of clinical risk factors enhances the performance of BMD in the prediction of hip and osteoporotic fractures in men and women

J. A. Kanis · A. Oden · O. Johnell · H. Johansson · C. De Laet · J. Brown · P. Burckhardt · C. Cooper · C. Christiansen · S. Cummings · J. A. Eisman · S. Fujiwara · C. Glüer · D. Goltzman · D. Hans · M.-A. Krieg · A. La Croix · E. McCloskey · D. Mellstrom · L. J. Melton III · H. Pols · J. Reeve · K. Sanders · A-M. Schott · A. Silman · D. Torgerson · T. van Staa · N. B. Watts · N. Yoshimura

Received: 7 December 2006 / Accepted: 19 January 2007 / Published online: 24 February 2007

Abstract
Summary BMD and clinical risk factors predict hip and other osteoporotic fractures. The combination of clinical risk factors and BMD provide higher specificity and sensitivity than either alone.
Introduction and hypotheses To develop a risk assessment tool based on clinical risk factors (CRFs) with and without BMD.
Methods Nine population-based studies were studied in which BMD and CRFs were documented at baseline. Poisson regression models were developed for hip fracture and other osteoporotic fractures, with and without hip BMD. Fracture risk was expressed as gradient of risk (GR, risk ratio/SD change in risk score).
Results CRFs alone predicted hip fracture with a GR of 2.1/SD at the age of 50 years and decreased with age. The use of BMD alone provided a higher GR (3.7/SD), and was improved further with the combined use of CRFs and BMD (4.2/SD). For other osteoporotic fractures, the GRs were lower than for hip fracture. The GR with CRFs alone was 1.4/SD at the age of 50 years, similar to that provided by BMD (GR=1.4/SD) and was not markedly increased by the combination (GR=1.4/SD). The performance characteristics of clinical risk factors with and without BMD were validated in eleven independent population-based cohorts.
Conclusions The models developed provide the basis for the integrated use of validated clinical risk factors in men and women to aid in fracture risk prediction.

Keywords Bone mineral density · Hip fracture · Meta-analysis · Osteoporotic fracture · Risk assessment

J. A. Kanis (✉) · E. McCloskey
WHO Collaborating Centre for Metabolic Bone Diseases,
University of Sheffield Medical School,
Beech Hill Road,
Sheffield S10 2RX, UK
e-mail: w.j.Pontefract@shef.ac.uk

A. Oden · H. Johansson
Consulting Statistician,
Gothenburg, Sweden

O. Johnell
Department of Orthopaedics,
Malmö General Hospital,
Malmo, Sweden

C. De Laet
Scientific Institute of Public Health,
Brussels, Belgium

J. Brown
Department of Rheumatology,
Sans Ospedale University de Quebec,
Quebec, Canada

P. Burckhardt
Department of Medicine,
CHUV University Hospital,
Lausanne, Switzerland

Introduction

Osteoporosis is operationally defined in terms of bone mineral density (BMD) [1]. Against this background, the clinical development of pharmaceutical agents has focussed on the selection of patients on the basis of low BMD for inclusion into trials of efficacy [2, 3]. As a consequence, guidance on therapeutic intervention has also emphasised the assessment of BMD [4–8]. In Europe, for example, women with clinical risk factors are considered for treatment where the T-score for BMD lies below the diagnostic threshold of osteoporosis, a T-score of −2.5 or less [4, 5]. Elsewhere, different T-score thresholds are used [6, 8].

The risk of fracture is, however, multi-factorial and many independent risk factors have been identified that contribute to risk over and above that reflected by BMD [9]. Their consideration along with BMD in the assessment of fracture risk increases the sensitivity of the test without sacrificing specificity [9]. In other words, the higher the gradient of risk (GR) of the test (the increase in fracture risk per standard deviation increase in risk score), the more accurately the individuals who will fracture are identified so that the overall risk in the group identified will be higher [10]. This has the effect of improving the cost-effectiveness of treatment.

Over the past several years, a series of meta-analyses has been performed to identify clinical risk factors for fracture and to determine their dependence upon age, sex and BMD [11–

C. Cooper
MRC Epidemiology Unit, Southampton General Hospital,
Southampton, UK

C. Christiansen
CCBR,
Ballerup, Denmark

S. Cummings
SF Coordinating Center,
San Francisco, CA, USA

J. A. Eisman
Bone and Mineral Research Program,
Garvan Institute of Medical Research,
St Vincent's, Hospital and University of New South Wales,
Sydney, Australia

S. Fujiwara
Department of Clinical Studies,
Radiation Effects Research Foundation,
Hiroshima, Japan

C. Glüer
Medizinische Physik, Universitas Klinikum Schleswig-Hostein,
Keil, Germany

D. Goltzman
Department of Medicine, McGill University,
Montreal, Canada

D. Hans
Nuclear Medicine Division, Geneva University Hospital,
Geneva, Switzerland

M.-A. Krieg
CHUV University Hospital,
Lausanne, Switzerland

A. La Croix
Fred Hutchinson Cancer Research Center,
Seattle, USA

D. Mellstrom
Department of Geriatric Medicine,
Goteborg University,
Gothenburg, Sweden

L. J. Melton III
Division of Epidemiology, Mayo Clinic,
Rochester, MN, USA

H. Pols
Department of Internal Medicine,
Erasmus Medical Centre Rotterdam,
Rotterdam, The Netherlands

J. Reeve
Strangeway's Research Laboratory, Wort's Causeway,
Cambridge, UK

K. Sanders
Department of Clinical and Biomedical Sciences,
University of Melbourne,
Barwon Health, Australia

A-M. Schott
INSERM U831, Hospices Civils de Lyon,
Lyon, France

A. Silman
ARC Epidemiology Unit,
University of Manchester,
Manchester, UK

D. Torgerson
Department of Health Sciences, University of York,
Yorkshire, UK

T. van Staa
Department of Pharmaco-epidemiology and Pharmacotherapy,
University of Utrecht,
Holland, The Netherlands

N. B. Watts
University of Cincinnati College of Medicine,
Cincinnati, OH, USA

N. Yoshimura
Joint Disease Research,
Graduate School of Medicine,
University of Tokyo,
Tokyo, Japan

19]. These analyses were based on the individual data from prospective population-based studies carried out at different centres around the world. Access to the primary data permits the inter-dependence of each of the candidate risk factors to be examined so that they can be combined for clinical use. The aim of this study was to utilise these data to determine the impact of the addition of multiple clinical risk factors to BMD for the prediction of fractures, and to validate the findings using data from independent cohorts.

Methods

Primary cohorts

We used baseline and follow-up data from nine prospective population-based cohorts comprising the Rotterdam Study, the European Vertebral Osteoporosis Study (later the European Prospective Osteoporosis Study (EVOS/EPOS), the Canadian Multicentre Osteoporosis Study (CaMos), Rochester, Sheffield, the Dubbo Osteoporosis Epidemiology Study (DOES), a cohort from Hiroshima and two cohorts from Gothenburg. Details of each of the cohorts are published elsewhere, but are summarised briefly below and in Tables 1 and 2.

The Rotterdam Study, begun in 1990, is an ongoing prospective cohort study that aimed to examine and follow-up all residents aged 55 years and older living in Ommoord, a district of Rotterdam [20]. By 1993 7,983 residents had been included (response rate 78%). Fracture follow-up was achieved through an automatic link with general practitioner computer systems and hospital admission data [21]. Fracture data were collected and validated by two independent research physicians. For this analysis, validated fracture follow up was available for 6,851 participants (2,793 men) with an average follow-up time of 6 years. Femoral neck BMD was measured in 5,731 individuals (2,414 men) by DXA (Lunar DPX-L).

The European Vertebral Osteoporosis Study (EVOS) comprised age- and sex-stratified random samples from 36 centres in 19 European countries [22]. Equal numbers of men and women were drawn in each centre within six 5-year age bands (50–74 and 75+ years). BMD was measured in 3,461 men and women from 13 centres by DXA at the femoral neck using pencil beam machines that were cross-calibrated using the European Spine Phantom. This sample provided the framework for the European Prospective Osteoporosis Study (EPOS) where repeated assessment was undertaken in 29 of the centres [23, 24]. For this analysis, validated fracture follow up was available for

Table 1 Details of the cohorts studied

Cohort	Number	% female	Person-years	Hip fracture	Other osteoporotic fracture	Age (mean)	Age range
(a) Primary cohorts							
EVOS/EPOS	13,490	52	40,681	50	719	64	40–95
CaMos	9,101	69	25,834	40	307	62	25–103
Rochester	1,001	65	6,227	42	244	57	21–94
Rotterdam	6,851	59	39,593	220	646	69	55–106
DOES	2,089	61	15,994	103	407	71	57–96
Gothenburg II	1,970	59	15,201	271	350	78	20–89
Hiroshima	2,603	70	9,825	32	90	65	47–95
Sheffield	2,170	100	6,894	63	243	80	74–96
Gothenburg I	7,065	100	29,603	29	312	59	69–86
Totals	4,6340	68	189,852	850	3,318	65	
(b) Validation cohorts							
THIN	135,695	100	606,822	1336	4,802	60	50–116
SOF	5,251	100	57,388	523	1,313	71	65–99
York	3,409	100	5,927	35	195	77	48–99
Geelong I	1,173	100	7,315	32	143	62	35–95
Geelong II	1,865	100	-[a]	73	443	63	35–95
OPUS	2,155	100	4,161	6	100[b]	67	55–80
PERF	5,415	100	39,096	58	801	64	43–81
EPIDOS	7,435	100	26,665	302	642	81	70–100
Miyama	353	53	3,173	7	44	59	40–79
SEMOF	6,721	100	18,712	73	581[b]	75	70–91
WHI	61,014	100	439,296	915	6,250[b]	66	50–79
Totals	230,486	100	1,208,528	3360	15,183	63	

[a] Case control study; [b] Any osteoporotic fracture.

Table 2 Risk factors and their prevalence by cohort

Cohort	BMI	BMD	Family history	Glucocorticoids	Prior fracture	Smoking	Alcohol	Rheumatoid arthritis
(a) Primary cohorts								
EVOS/EPOS	27.0	+	9	5	36	20	–	–
CaMos	26.9	+	–	5	44	–	3	6
Rochester	26.1	+	–	3	18	–	–	–
Rotterdam	26.3	+	8	2	14	23	23	–
DOES	25.6	+	–	6	13	7	16	3
Gothenburg I	25.4	–	–	–	9	16	–	–
Gothenburg II	24.6	–	4	4	18	25	–	–
Hiroshima	23.0	+	–	3	26	20	–	–
Sheffield	26.7	+	5	9	51	7	–	2
Totals	26.2		7	4	29	20	11	5
(b) Validation cohorts								
THIN	26.0	–	–	2	10	40[c]	32	1
SOF	26.4	+	15	12	35	11	4	7
York	25.0[a]	–	9[b]	3	40	9	–	–
Geelong I	24.8	+	8	3	15	12	8	11
Geelong II	24.1	+	10	13	32	16	4	15
OPUS	26.6	+	11	3	44	14	3	7
PERF	25.5	+	–	–	16	–	–	–
EPIDOS	25.4	+	9	6	40	3	3	–
Miyama	22.1	+	–	0	32	27	14	–
SEMOF	28.9	+[d]	10[6]	4	51	8	<1	–
WHI	28.4	+[e]	13	1	17	7	4	5
Totals	26.7		12	2	16	27	21	3

[a] Height assumed to be 1.6 m; [b] Maternal history of hip fracture; [c] Ever smoking, [d] subset of 820 women, [e] subset of 4,193 women.

13,490 participants (6,521 men) with an average follow-up time of 3 years. Femoral neck BMD was measured in 4,746 individuals (2,141 men).

The Canadian Multicentre Osteoporosis study (CaMos) is an ongoing prospective age stratified cohort. The study is documenting the incidence of fractures and risk factors in a random sample of 9,424 men and women aged 25 years or more selected by telephone listings. The sampling frame is from nine study centres in seven provinces [25]. Characterisation of individuals was by interview. BMD was measured by DXA at the femoral neck with Hologic QDR in seven centres and the Lunar DPX Alpha in two centres in 8,297 individuals (2,589 men). Machines were cross-calibrated using the same European Spine Phantom. For this analysis, validated fracture follow-up was available for 9,101 participants (2,801 men) with an average follow-up time of 3 years.

The Rochester cohort was recruited from two random population samples stratified by decade of age, one of women who were subsequently followed for up to 20 years [26], and another sample of women and men followed for 8 years [27]. BMD of the right femoral neck was measured by dual photon absorptiometry in the first cohort (cross-calibrated to DXA) and by DXA (Hologic QDR 2000) in the second group. Fractures were ascertained by periodic interview combined with review of the in-patient and out-patient medical records of all local care providers. For this analysis, validated fracture follow up was available for 1001 participants (348 men) with an average follow-up time of 6 years. Femoral neck BMD was measured in 993 individuals (345 men).

The Sheffield cohort comprised women aged 75 years or more selected randomly from the population of Sheffield, UK and surrounding districts between 1993 and 1999. Approximately 35,000 women, identified from general practitioner listings, were contacted by letter and invited to attend for the assessment of skeletal status; 5,873 women were willing to attend. Of these, 281 women were excluded and the remainder randomly allocated to treatment with placebo or the bisphosphonate, clodronate, to study its effects on fracture risk. The material for this study comprised 2,172 women allocated to treatment with placebo only [28, 29]. All women had baseline assessment of BMD undertaken at the femoral neck using the Hologic QDR 4500. Outcomes were assessed by 6-monthly home visits. For this analysis, validated fracture follow up was

available for 2,170 participants with an average follow-up time of 6 years. Femoral neck BMD was measured in 2,150 individuals.

The Dubbo Osteoporosis Epidemiology Study (DOES) is a population-based study with multiple assessments of skeletal status in men and women aged 60 years or more from Dubbo, Australia [30]. Participation in the study was 56% of the population. Baseline measurements included BMD at the femoral neck assessed using DXA (GE-Lunar, DPX and Prodigy). Fractures are identified through radiologists' reports from the two centres servicing the region. For this analysis, validated fracture follow-up was available for 2,089 participants (819 men) with an average follow-up time of 8 years. Femoral neck BMD was measured in 2,060 individuals (801 men).

The Gothenburg I study comprised four birth cohorts of 2375 randomly sampled men and women aged 70 years or more followed for up to 20 years after a baseline BMD measurement [31]. The participants were drawn randomly from the population register in Gothenburg by the date of birth to provide cohorts aged 70, 76, 79 and 85 years at the time of investigation. The participation rate was 73%. Bone mineral density was measured at the right heel using dual photon absorptiometry. For this analysis, validated fracture follow-up was available for 1,970 participants (812 men) with an average follow-up time of 8 years. Since BMD was measured at a peripheral site, data were not used in models including BMD.

The Gothenburg II study comprised a randomly drawn population cohort of over 7,000 women aged 50–70 years followed for 4 years [32]. The participation rate was 67%. Assessment included a standardised questionnaire that recorded information on risk factors for osteoporosis. Fractures were identified prospectively through the radiology departments servicing the region. BMD was assessed at baseline at the distal forearm by using the Osteometer DTX-200. For this analysis, validated fracture follow-up was available for 7065 participants with an average follow-up time of 4 years. Since BMD was measured at a peripheral site, BMD data were not included in models adjusting for BMD.

The Adult Health Study (AHS) was established in 1958 to document the late health effects of radiation exposure among atomic bomb survivors in Hiroshima and Nagasaki. The original AHS cohort consisted of about 15,000 atomic bomb survivors and 5,000 controls selected from residents in Hiroshima and Nagasaki using the 1950 national census supplementary schedules and the Atomic Bomb Survivors Survey. AHS subjects have been followed through biennial medical examinations since 1958. The participation rate has been around 80% throughout this period. BMD was measured at the proximal femur by DXA in 1994 (Hologic QDR 2000) in 2,588 individuals (791 men). Self-reported fractures were documented at 6-monthly intervals [33, 34]. For this analysis, validated fracture follow-up was available for 2,603 participants (793 men) with an average follow-up time of 4 years.

Validation cohorts

The performance characteristics determined from the primary cohorts were evaluated in eleven independent population based cohorts that did not participate in the model synthesis. These comprise the Epidemiologie de l'osteoporose (EPIDOS) study (France), the Study of Osteoporotic Fractures (SOF) in the US, two cohorts from the Geelong osteoporosis study in Australia, the OPUS study drawn from 5 European countries, the Prospective Epidemiological Risk Factors (PERF) study from Denmark, the Health Improvement Network (THIN) data-base in the UK, the SEMOF Study from Switzerland, the Women's Health Initiative (US), a cohort from York, UK and a cohort from Miyama in Japan. The characteristics of the cohorts are shown in Tables 1 and 2, and described briefly below.

The EPIDOS study comprises a population based cohort of women aged 75 years or more from five French centres (Amiens, Lyon, Mont Pellier, Paris and Toulouse) [35]. Between April 1992 and December 1993, 7,598 women were recruited through mailings using large population-based listings such as voter registration rolls. Baseline characteristics were obtained through a structured questionnaire, as well as through clinical and functional examinations, and BMD at the femoral neck assessed by DXA (Lunar DPX). Information on fracture outcomes was obtained through direct contact with the study participants at 4-monthly intervals or from a family member or the individuals' physicians. For this analysis, validated fracture follow-up was available for 7,435 women. Femoral neck BMD was measured in 7,402 individuals.

The PERF study was a population based cohort originally comprising 8,502 postmenopausal women aged 45–70 years recruited between the years 1977–1997 [36]. The survey invited women to participate in screening for various placebo controlled clinical trials and epidemiological studies at Copenhagen. Between the years 2000–2001 individuals were recalled for a follow-up examination. Follow-up information was obtained in 6,573 women (77.3%). Of the clinical risk factors information was only available for a history of prior fracture. Incident fractures were documented from spinal radiographs and personal history. Validated follow-up information was available in 5,415 women.

The THIN research database contains computerised records of general practitioners, similar to the General Practice Research Database [37]. The study population comprised all women aged 50 years or more registered with

a general practice that contributed data to THIN (N= 366,104) with an average follow-up of 5.8 years. Information on the relevant clinical risk factors was available in 135,695 women (BMI and smoking history were not recorded in all patients). No information was available for a parental fracture history, and smoking history was for 'ever' rather than 'current smoking'. BMD tests are not ultimately undertaken in UK general practice. Fracture ascertainment was from the general practitioner records.

The OPUS study comprises five age-stratified population-based female cohorts drawn from different European centres (Sheffield and Aberdeen (UK), Berlin and Kiel (Germany), and Paris (France)). Participants completed a questionnaire at baseline and BMD was measured by DXA at the femoral neck using the Hologic QDR 4500 (Kiel, Paris and Sheffield) or the Lunar Expert (Aberdeen and Berlin). Baseline estimates for BMD were available in 2155 women [38].

The York cohort [39] was based on a study of hip protectors. The cohort comprised women aged 70 years and over drawn from general practice lists. Baseline characteristics on clinical risk factors were available in 3,409 individuals, most of whom participated in the randomised study of hip protectors. The study showed no significant effect of hip protectors on the risk of hip fracture (OR= 1.17; 95% CI=0.78–1.75). Information on alcohol intake or the presence of rheumatoid arthritis was not available. Weight but not height was available, and we assumed a height of 1.6 m for the calculation of BMI.

The SOF is a multicentre cohort study of risk factors for osteoporosis and fracture in 9,704 elderly women [40]. Participants were ambulatory, Caucasian and aged 65 years or older when recruited between September 1986 and October 1988 at four clinical centres from the USA (Baltimore, Minneapolis, Pittsburgh and Portland). Baseline characteristics were obtained through a structured questionnaire and BMD was assessed during 1990–1991 at the femoral neck using the Hologic QDR 1000. Fractures were assessed by telephone or correspondence at four monthly intervals and confirmed from X-ray reports.

The Geelong Osteoporosis study comprises two cohort studies of women drawn from Geelong and surrounding districts in south east Australia (population 222,000). Two cohorts were available for study [41]. The first (Geelong I) was an age-stratified sample of women drawn randomly from the electoral roll. Women underwent a baseline assessment between 1994 and 1997 to ascertain risk factors and BMD at the femoral neck (Lunar DPX-L). Fractures were radiographically confirmed from hospital records and deaths confirmed from the Australian Institute of Health and Welfare.

The second cohort (Geelong II) was a case-control study [41]. Cases comprised patients aged 35 years or more identified with an incident fracture by weekly database searching of the radiological practices in the region between 1994 and 1996. All women identified with incident fractures were invited to attend for assessment. Ten percent of women died during the ascertainment period and 11% were unable to give informed consent. A total of 692 cases were studied with an acceptance rate of 77%. The control group comprised the women in Geelong I who did not sustain an incident fracture between 1994 and 1996. Both cases and controls were interviewed by means of a structured questionnaire, and BMD was measured at the femoral neck by DXA (Lunar DPX-L). In cases, BMD was measured on the side contra-lateral to the fracture.

The Miyama study is a population-based cohort drawn from inhabitants born in Miyama, Japan between 1910 and 1949 as compiled in 1989 [42]. Of 1543 inhabitants, an age-stratified sample of 400 men and women was drawn by birth decade. A baseline questionnaire was administered in 1990 and BMD was measured at the femoral neck (Lunar DPX) and data available in 353 individuals. Reviews were undertaken in 1993, 1997 and 2000.

The Swiss Evaluation of the Methods of Measurement of Osteoporotic Fracture Risk (SEMOF) study is a prospective multicentre (10 centres) study, the aims of which were to compare the performance characteristics of different ultrasound technologies [43]. 60,000 women aged 70 years or more were randomly selected from an address register and 7,609 women agreed to participate in the study. Six thousand seven hundred and twenty-one women completed a questionnaire and were prospectively studied for a mean time of 2.9 years. Incident fracture was recorded by questionnaire administered at 6 monthly intervals and confirmed from medical records. BMD at the femoral neck (Hologic QDR 4500) was measured in 820 women.

The Women's Health Initiative (WHI) study comprises three overlapping randomised controlled studies and an observational study in post-menopausal women aged 50–79 years [44, 45]. The trials comprised dietary modification with low fat (n=48,836), hormone replacement therapy (HRT) in women with or without a uterus (n=27,347), and supplementation with calcium and vitamin D (n=36,282). The total sample size was 161,808. For this analysis, women less than 55 years were excluded since a history of prior fracture was not available. So too were women taking bone active medication (HRT, bisphosphonates, calcitonin), leaving a sample size of 61,014. Bone mineral density measurements at the femoral neck took place at few centres and were available in 4,193 women using the Hologic 2000. Hip fractures were documented from medical records and adjudicated at a central facility. In the clinical trials, other fractures were adjudicated locally and in the observational study by self report. In the subgroup in whom BMD was measured, non-hip fractures were locally adjudicated.

Baseline and outcome variables

Height and weight were measured using standard techniques in all cohorts. Body mass index (BMI) was calculated as weight in kg divided by height squared in metres and used as a continuous variable. BMD was assessed at the femoral neck by DXA with the exception of the two Gothenburg cohorts. Femoral neck BMD was used as a continuous variable (cohort specific Z-scores excluding the two cohorts from Gothenburg). The clinical risk factors utilised were those identified from previous meta-analyses. These comprised a parental history of hip fracture [11], exposure to systemic glucocorticoids [12], a prior history of fragility fracture [13], current smoking [18], high intake of alcohol (>2 units daily on average) [16] and the presence of rheumatoid arthritis [12]. The prevalence of the risk factors are shown in Table 2. Note that not all primary cohorts nor validation cohorts had complete information.

Fracture ascertainment in the primary cohorts was undertaken by self-report (Sheffield, EVOS/EPOS, Hiroshima) and/or verified from hospital or central databases (Gothenburg, CaMos, DOES, Sheffield, EVOS/EPOS, Rochester, Rotterdam). The EPOS and the Rotterdam study also included sequential systematic radiography to define incident morphometric vertebral fractures, but these were not used in this analysis. In the analysis, we used information on fractures considered to be osteoporotic. In addition, hip fracture alone was considered separately. An osteoporotic fracture was one considered to be due to osteoporosis by the investigator in the EVOS/EPOS study and in CaMos. For the EVOS/EPOS study, osteoporotic fractures comprised hip, forearm, humeral or spine fractures. For the CaMos Study they comprised fractures of the spine, pelvis, ribs, distal forearm, forearm and hip. In the other cohorts, fractures at sites considered to be characteristic for osteoporosis were extracted [46].

Fractures were documented in the validation cohorts by self-report (Miyama, PERF cohort details) and/or verified from hospital, general practitioner or individual imaging databases (EPIDOS, York, THIN, Geelong I and II, PERF, SEMOF) and other cohorts.

Statistical methods

The association of risk factors with the risk of hip and other osteoporotic fracture was examined using a Poisson regression model in each cohort separately. Covariates included current age and time since start of follow-up, and analyses were performed for both sexes separately with and without taking BMD information into account. BMD was expressed as sex- and cohort-specific Z-scores. BMI was analysed continuously. The β-coefficients for each covariate of each cohort and the two sexes were weighted according to the variance, and merged to determine the weighted mean of the coefficient and its standard deviation. The risk ratios at different BMI or BMD levels are then given by $e^{(\text{weighted mean coefficient})}$.

For each risk factor, all significant interactions terms that were identified by the previous meta-analyses were entered (with age, time, sex and the risk factor) with and without BMD. Interactions that were significant for hip fracture risk were also entered into the model for other osteoporotic fractures. Where interactions noted in the "mega-analyses" were no longer significant for hip fracture and other osteoporotic fractures, these were omitted in a step-wise manner by dropping the interaction with the largest p value. Take, for example, the interaction of BMD and age for hip fracture risk: hip fracture risk prediction was significantly higher with BMD at younger ages [14] and the higher predictive values persisted when entered into the model. The respective β functions for the interaction (BMD · current age) were retained in both the model for hip fracture and other osteoporotic fracture, though this fell short of significance in the model for other osteoporotic fractures ($p=0.074$). Conversely, for BMI, a significant interaction was noted with age in the meta-analysis (i.e., an increase in risk ratio of low BMI for osteoporotic fracture with age) [15], but was no longer significant in any model, and the interaction term was dropped from the hazard functions for fracture. The other interactions that were retained were age · sex, BMD · age, BMD · BMD, family history · age, prior fracture · age, BMI · BMI, and age · age.

Complete information from all cohorts used in the model were available for the continuous variables (BMI and BMD) though BMD was not used in the cohorts from Gothenburg, since BMD was not measured at the femoral neck. Not all cohorts had complete information on all the dichotomous risk factors (see Table 2). For example, a current history of smoking was not available from CaMos and Rochester. When one dichotomous variable (e.g., smoking) was deleted from the model this had a very minor effect on the β coefficients for the other variables. Since these deletions had little or no effect, the original β coefficients were used.

The performance of the original model was assessed as the gradient of risk, i.e., the increase in fracture risk per SD increase in risk score. Gradients of risk were computed for the prediction of hip fracture and other major osteoporotic fractures (clinical spine, forearm, proximal humerus) with BMD alone, the clinical risk factors alone, and the combination. The distribution of risk score was examined using the Edgeworth expansion [47].

Heterogeneity between cohorts was tested by means of the I^2 statistic [48]. Moderate heterogeneity was noted for hip fracture outcomes with and without BMD ($I^2=56\%$ and

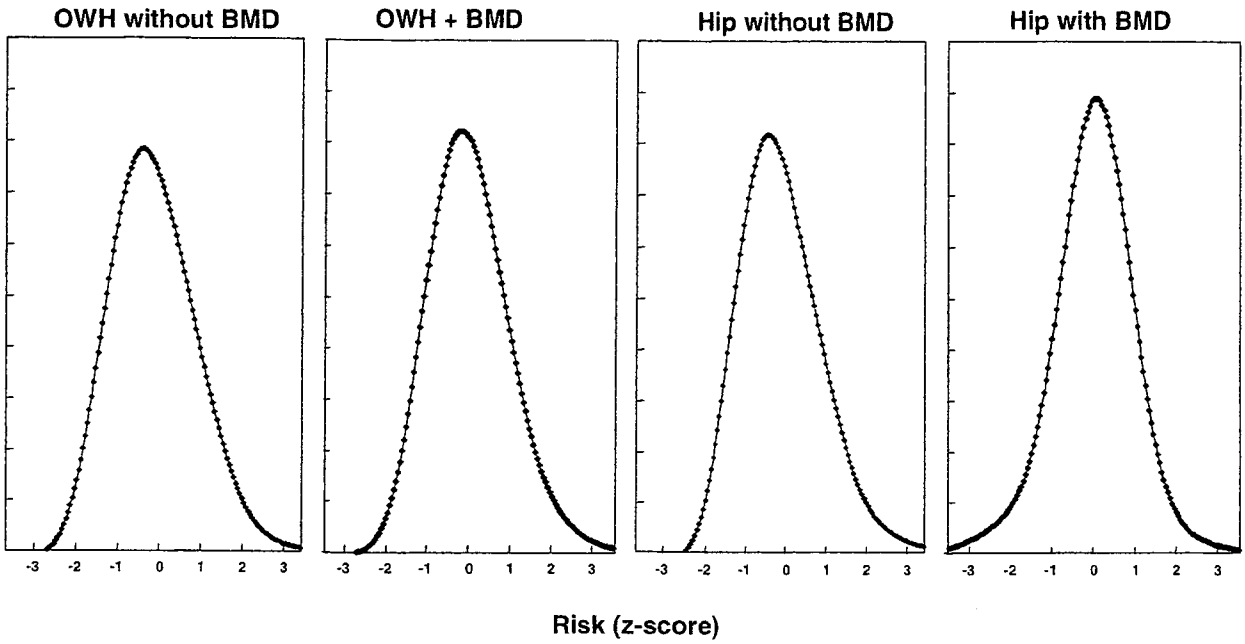

Fig. 1 Distribution of risk scores with and without BMD. OWH refers to osteoporotic fractures without hip fracture

64%, respectively; $P<0.05$) and high heterogeneity for other fracture outcomes ($I^2=83\%$ and 82%, respectively; $P<0.001$). When the interaction between risk score and current age (risk score· age) was included, there was less marked heterogeneity between cohorts for the risk score for hip fracture with or without BMD ($I^2=66\%$ and 60%, respectively) and for other osteoporotic fractures ($I^2=52\%$ and 47%, respectively).

For each validation cohort, the computed risk score was expressed as a sex-specific Z-score. The gradient of hip fracture and other osteoporotic fracture risk was examined for the use of the clinical risk factors alone and in combination with BMD. Gradients of risk were also transformed as area under the receiver operating characteristic (ROC) curve (AUC) as detailed in the Appendix.

Results

The primary cohorts comprised 46,340 men and women (68% female) followed for approximately 190,000 person-years. During follow-up, 4,168 osteoporotic fractures were documented of which 850 were at the hip. The prevalence of the risk factors is shown in Table 2 and the distribution of risk scores shown in Fig. 1. The performance characteristics of the models are given in Table 3 expressed as

Table 3 Gradients of risk per SD change in risk score (with 95% confidence intervals) with the use of BMD, clinical risk factors or the combination

Age	Gradient of risk		
	BMD only	Clinical risk factors alone	Clinical risk factors + BMD
(a) Hip fracture			
50	3.68 (2.61–5.19)	2.05 (1.58–2.65)	4.23 (3.12–5.73)
60	3.07 (2.42–3.89)	1.95 (1.63–2.33)	3.51 (2.85–4.33)
70	2.78 (2.39–3.23)	1.84 (1.65–2.05)	2.91 (2.56–3.31)
80	2.28 (2.09–2.50)	1.75 (1.62–1.90)	2.42 (2.18–2.69)
90	1.70 (1.50–1.93)	1.66 (1.47–1.87)	2.02 (1.71–2.38)
(b) Other osteoporotic fractures			
50	1.19 (1.05–1.34)	1.41 (1.28–1.56)	1.44 (1.30–1.59)
60	1.28 (1.18–1.39)	1.48 (1.39–1.58)	1.52 (1.42–1.62)
70	1.39 (1.30–1.48)	1.55 (1.48–1.62)	1.61 (1.54–1.68)
80	1.54 (1.44–1.65)	1.63 (1.54–1.72)	1.71 (1.62–1.80)
90	1.56 (1.40–1.75)	1.72 (1.58–1.88)	1.81 (1.67–1.97)

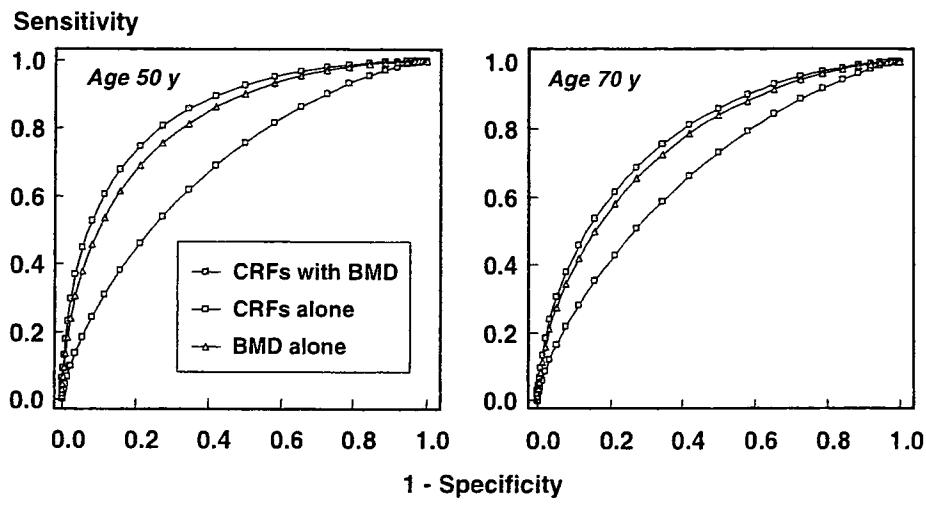

Fig. 2 Receiver operating characteristic curves for the risk score for hip fracture prediction at the ages of 50 and 70 years. CRF = clinical risk factor

gradients of risk per SD change in the risk indicator. Note that the category of other osteoporotic fracture excludes hip fracture, whereas hip fracture was included in the previously published meta-analyses under the term "any osteoporotic fracture".

For hip fracture prediction, gradients of risk decreased with age, as did the AUC of the ROC curve (Fig. 2). At all ages, BMD outperformed the clinical risk factors alone, except at the age of 90 years (Table 3). When BMD was combined with the clinical risk factors there was an increment in the GR/SD. For example, hip fracture risk increased by 3.7/SD decrease in femoral neck BMD at the age of 50 years, and by 2.1/SD with the use of clinical risk factors, but their combined use gave a GR of 4.2/SD. For the prediction of other osteoporotic fractures, GR/SD with BMD were, as expected, lower than for the prediction of hip fracture. GR varied from 1.2 to 1.6/SD depending on age and tended to increase with age, in contrast to the prediction of hip fracture. When clinical risk factors alone were used, the GR also increased with age and, unlike for hip fracture prediction, the use of clinical risk factors outperformed BMD. As in the case of hip fracture prediction, there was an increment in GR when the clinical risk factors were used in combination with BMD. The increment in GR using BMD alone and in conjunction with clinical risk factors was, however, more substantial in the case of hip fracture prediction than for the prediction of other osteoporotic fractures.

The performance characteristics of the validation cohorts are shown in Table 4. Since gradients of risk were age-

Table 4 Gradient of risk/SD change in risk score of the validation cohorts compared to the original cohorts standardised to the age of 70 years (±95% confidence estimates)

	Hip fractures		Other osteoporotic fractures	
Cohort	Without BMD	With BMD	Without BMD	With BMD
Geelong I	1.88 (1.07–3.29) [0.67]	1.71 (0.74–3.96) [0.65]	1.34 (1.12–1.61) [0.58]	1.57 (1.31–1.88) [0.63]
Geelong II	1.50 (1.05–2.13) [0.61]	3.40 (1.99–5.80) [0.81]	1.30 (1.14–1.48) [0.57]	1.54 (1.36–1.76) [0.62]
OPUS	2.48 (1.26–4.91) [0.74]	2.09 (0.98–4.47) [0.70]	1.32 (1.08–1.62) [0.58]	1.38 (1.15–1.65) [0.59]
York	2.05 (1.13–3.72) [0.69]	– [–]	1.74 (1.37–2.21) [0.65]	– [–]
PERF	1.28 (1.01–1.62) [0.57]	2.72 (1.43–5.16) [0.76]	1.14 (1.05–1.23) [0.54]	1.19 (1.05–1.35) [0.55]
SOF	1.58 (1.34–1.87) [0.63]	2.21 (1.79–2.73) [0.71]	1.24 (1.15–1.34) [0.56]	1.31 (1.20–1.42) [0.58]
THIN	1.54 (1.45–1.63) [0.62]	– [–]	1.29 (1.26–1.32) [0.57]	– [–]
EPIDOS	1.70 (1.18–2.44) [0.65]	2.89 (1.98–4.21) [0.77]	1.41 (1.11–1.78) [0.60]	1.47 (1.17–1.86) [0.61]
Miyama	2.87 (0.98–8.37) [0.77]	3.07 (0.97–9.64) [0.79]	3.50 (2.42–5.07) [0.81]	2.80 (2.06–3.80) [0.77]
SEMOF	1.76 (1.03–3.01) [0.65]	2.18 (1.27–3.74) [0.71]	1.32 (1.10–1.58) [0.58]	1.44 (1.16–1.79) [0.60]
WHI	1.54 (1.43–1.66) [0.62]	2.44 (1.85–3.21) [0.74]	1.26 (1.23–1.29) [0.56]	1.46 (1.35–1.58) [0.60]
Original cohorts	1.84 (1.65–2.05) [0.67]	2.91 (2.56–3.31) [0.78]	1.55 (1.48–1.62) [0.62]	1.61 (1.54–1.68) [0.63]

AUC's under the ROC curve are shown in square brackets.

dependent, these were standardised to the age of 70 years. Note that when one or more risk factor was unavailable from the validation cohorts, the gradient of risk was still computed from the original model, but with a β value of zero for that particular risk factor. Table 4 also shows areas under the ROC curve. Gradients of risk and AUC's were comparable in the validation cohorts compared with the original cohorts. For example, for hip fracture prediction without BMD, the mean AUC was 0.66 in the validation cohorts compared with 0.67 in the original cohorts. With the addition of BMD the mean AUC was 0.74 and 0.78, respectively. For other osteoporotic fractures the mean AUC was 0.60 in the validation cohorts and 0.62 in the original cohorts, excluding BMD. With the addition of BMD, the average AUCs were 0.62 and 0.63, respectively.

Discussion

The principal finding of this study is that the use of clinical risk factors alone provides some discriminative value in the categorisation of fracture risk. However, the addition of bone mineral density improves the GR/SD still further. For hip fracture prediction, the GR was markedly improved at younger ages, whereas little age dependency was seen for the prediction of other osteoporotic fractures.

In this analysis, we chose to provide independent models for hip fracture and for other osteoporotic fractures. The principal reason is that, although many risk factors, including those chosen here are common for both fracture types, the risk ratios differ and are generally higher for hip fracture than for other osteoporotic fractures [11–19]. It is possible that the strength of risk factors also varies between the different types of osteoporotic fracture, but much larger material than currently available would be required to incorporate this with accuracy into the model. The available evidence would suggest that, with the exception of falls, risk factors for vertebral fracture do not differ substantially from those from other osteoporotic fractures [49–52].

The use of clinical risk factors alone provided a GR/SD that lay between 1.4 and 2.1, depending upon age and the type of fracture predicted. These gradients are comparable to the use of BMD alone to predict fractures [14, 53]. For example, for the prediction of any osteoporotic fracture, the GR at the age of 70 years was 1.5 with femoral neck BMD [14]. With peripheral BMD the gradient of risk is somewhat, though not significantly lower (GR=1.4/SD; 95% CI=1.3–1.5/SD). These data suggest that clinical risk factors alone are of value and might be used, therefore, in the many countries where DXA facilities are sparse [54].

Notwithstanding the above, a further important finding is that there are substantial gains to be had in the use of the clinical risk factors in conjunction with BMD, particularly in the case of hip fracture prediction. At the age of 50 years, for example, the gradient of risk with BMD alone was 3.7/SD, but with the addition of clinical risk factors was 4.2/SD.

Although the improvement in GR with the addition of BMD was modest particularly in the case of other osteoporotic fractures, it should be recognised that gradients of risk are not multiplicative. For example, at the age of 70 years, BMD alone gave a GR of 2.8/SD for hip fracture. For the clinical risk factors the GR was 1.8/SD. If these two tests were totally independent, the combined GR would be $\sqrt{(2.8^2 + 1.8^2)} = 3.3$. The observed gradient of risk (2.9) falls short of the theoretical upper limit, since there was a significant correlation between the clinical risk factor score and BMD (r=0.25). The increment in gradient of risk for the prediction of other fractures was smaller, but there was also a significant correlation between the clinical risk factor score and BMD (r=0.10).

It is of interest that the GR for hip fracture prediction decreased with age. We have previously reported this for BMD alone [14], but in the present study, this was also evident with the use of clinical risk factors alone. It is possible that skeletal or extra-skeletal risk factors not measured, such as quality of bone or liability to falls, are captured by the risk factors included in the models that affect the GR. If so, the same cannot be said for the other osteoporotic fractures, which tended to be predicted more strongly with advancing age.

As discussed elsewhere [10, 55], increases in GR improve sensitivity without markedly affecting specificity for fracture prediction. For example, if it were appropriate to consider 10% of women aged 50 years to be at high risk, a test with a gradient of risk of 2.0/SD (i.e., the use of clinical risk factors alone) would be expected to have a sensitivity of 26% for a specificity of 91%. The same scenario, but with a test that gave a gradient of risk of 4.0 would increase greatly the sensitivity of the test to 42% without adverse effects on specificity (92%), and the positive predictive value would increase from 11% to 25%. Thus, modest improvements in GR have substantial effects on sensitivity and positive predictive value.

Several population-based studies have examined the relationship between risk factors with and without the inclusion of BMD [56–70]. With few exceptions these have not been validated in independent cohorts. An exception is a subset of the US-based SOF study which was used to produce a multivariate prediction model [57]. Twenty potential risk factors were considered in the model, both including and excluding BMD at the total hip. Age, weight and cigarette smoking appeared as independent risk factors, as did an indicator of physical condition (using the arms to stand from a chair). In addition, a history of maternal hip fracture after the age of 50 years and a history of prior